(Photo)physical Properties of New Molecular Glasses End-Capped with Thiophene Rings Composed of Diimide and Imine Units

Marzena Grucela-Zajac,[†] Katarzyna Bijak,[†] Slawomir Kula,[†] Michal Filapek,[†] Malgorzata Wiacek,[†] Henryk Janeczek,[‡] Lukasz Skorka,[§] Jacek Gasiorowski,[‖,⊥] Kurt Hingerl,[⊥] Niyazi Serdar Sariciftci,[‖] Natalia Nosidlak,[#] Gabriela Lewinska,[∇] Jerzy Sanetra,[∇] and Ewa Schab-Balcerzak*,[†,‡]

[†]Institute of Chemistry, University of Silesia, 9 Szkolna Street, 40-006 Katowice, Poland

[‡]Centre of Polymer and Carbon Materials, Polish Academy of Sciences, 34 M. Curie-Sklodowska Street, 41-819 Zabrze, Poland

[§]Faculty of Chemistry, Warsaw University of Technology, 3 Noakowskiego Street, 00-664 Warsaw, Poland

[‖]Linz Institute for Organic Solar Cells (LIOS), Physical Chemistry, and [⊥]Center for Surface and Nanoanalytics, Johannes Kepler University Linz, Altenberger Strasse 69, 4040 Linz, Austria

[#]Department of Electronics, AGH University of Science and Technology, Al. Mickiewicza 30, 30-059 Krakow, Poland

[∇]Institute of Physics, Cracow University of Technology, 1 Podchorazych Street, 30-035 Krakow, Poland

S *Supporting Information*

ABSTRACT: New symmetrical arylene bisimide derivatives formed by using electron-donating–electron-accepting systems were synthesized. They consist of a phthalic diimide or naphthalenediimide core and imine linkages and are end-capped with thiophene, bithiophene, and (ethylenedioxy)-thiophene units. Moreover, polymers were obtained from a new diamine, *N,N′*-bis(5-aminonaphthalenyl)naphthalene-1,4,5,8-dicarboximide and 2,5-thiophenedicarboxaldehyde or 2,2′-bithiophene-5,5′-dicarboxaldehyde. The prepared azomethine diimides exhibited glass-forming properties. The obtained compounds emitted blue light with the emission maximum at 470 nm. The value of the absorption coefficient was determined as a function of the photon energy using spectroscopic ellipsometry. All compounds are electrochemically active and undergo reversible electrochemical reduction and irreversible oxidation processes as was found in cyclic voltammetry and differential pulse voltammetry (DPV) studies. They exhibited a low electrochemically (DPV) calculated energy band gap (E_g) from 1.14 to 1.70 eV. The highest occupied molecular orbital and lowest unoccupied molecular orbital levels and E_g were additionally calculated theoretically by density functional theory at the B3LYP/6-31G(d,p) level. The photovoltaic properties of two model compounds as the active layer in organic solar cells in the configuration indium tin oxide/poly(3,4-(ethylenedioxy)thiophene):poly(styrenesulfonate)/active layer/Al under an illumination of 1.3 mW/cm^2 were studied. The device comprising poly(3-hexylthiophene) with the compound end-capped with bithiophene rings showed the highest value of V_{oc} (above 1 V). The conversion efficiency of the fabricated solar cell was in the range of 0.69−0.90%.
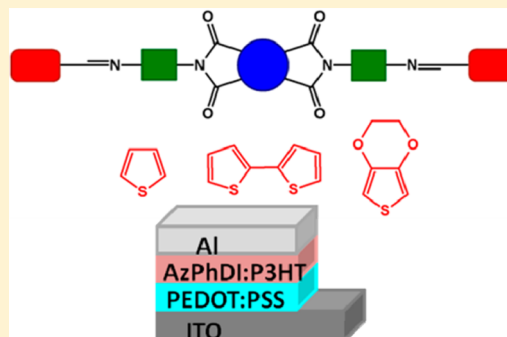
1. INTRODUCTION

During the past few decades, processable organic semiconductors, such as small molecules and conjugated polymers, have been intensively studied because of the easy tenability of optical and electrical properties by chemical synthesis. They are attractive for their potential applicability in the fabrication of different types of electronic devices, e.g., light-emitting diodes (LEDs), photodiodes (PDs), photovoltaic cells (PCs), or field effect transistors (FETs).[1−3] Although remarkable progress has been made, the development of highly efficient and long-term stable optical and electrical devices is still a challenge. Thus, it is necessary to design and synthesize processable conjugated polymers with expected properties such as a low band gap, a broad absorption range, a high charge mobility, and appropriate molecular energy levels.[4] Although polymers exhibit many

valuable properties suitable for the construction of optoelectronic devices, interest in low molecular weight semiconductors is growing due to their advantages of a well-defined molecular structure and molecular weight without any distribution and relatively easily purification. Among many low molar mass materials developed for optoelectronic applications, especially interesting are compounds that readily form glasses above room temperature and which are called molecular glasses or amorphous molecular materials.[5−9] Thus, they combine the characteristic properties of small molecules with the behavior of polymers, i.e., the ability to access amorphous solid states. They

may form uniform, transparent, and amorphous thin films by either vapor deposition or spin-coating methods in contrary to low molar mass compounds, which have a strong tendency for crystallization. Films from crystalline materials could be prepared only by using polymeric binders. Moreover, molecular glasses may show high thermal stability and high glass transition temperatures (T_g) which can be easily tuned by a subtle structural modification and can result in various T_g values. Among the currently investigated classes of materials, tetracarboxylic diimides have aroused a lot of attention due to the electron-deficient core leading to n-type (electron-transporting) semiconducting properties.[10] Although impressive progress has been made in developing electron-rich character (p-type) organic materials, semiconductors capable of electron transport are still challenges in the field of organic electronics.[10,11] Diimides considering the imide unit structure are divided into two kinds, that is, compounds with five- and six-membered imide rings, that is, phthalic diimides and naphthalene- and perylenediimides, respectively. A large number of either naphthalene or perylene tetracarboxylic diimides have been synthesized and investigated, and many of them have achieved high electron mobilities and air stability.[10,12,13] Naphthalene- and perylenediimides are studied as acceptor molecules in organic solar cells.[14−16] A study has been devoted to examining the linker effect at the N-position in a core-substituted diimide and such compounds given power conversion efficiencies between 0.01 and 0.48%. The authors used a phenyl linkage between thiophene and diimide through the N-position, which is also the scope of this paper, resulting in a 0.43% power conversion efficiency.[17] Researchers at the University of Washington[18] studied the effect of processing additives on the performance of naphthalenediimide acceptors, showing that when used with proper hole- and electron-blocking layers, naphthalenediimide-bearing device structures can reach a power conversion efficiency of 1.50%. Among perylenediimides there are two prominent studies, one of which was conducted by Bazan et al.[19] and was a comparative study where they used 7,7′-(4,4-bis(2-ethylhexyl)-4*H*-silolo[3,2-*b*:4,5-*b*′]dithiophene-2,6-diyl)bis(6-fluoro-4-(5′-hexyl-[2,2′-bithio-phen]-5-yl)benzo[*c*][1,2,5]thiadiazole) (*p*-DTS(FBTTh$_2$)$_2$) as the donor molecule and compared the acceptor behavior of PC$_{71}$BM and perylenediimide (PDI). Although PC$_{71}$BM showed higher efficiency of 7%, PDI showed a comparable power conversion efficiency of 3%, suggesting that solution-processable small molecules are promising candidates for photovoltaic applications. In the second study, Yao and co-workers[20] investigated the thienyl-linked PDI dimer and its photovoltaic properties, showing a 4.03% power conversion efficiency. On the other hand, five-membered imide rings, that is, phthalic diimides, are rather occasionally investigated as semiconductors.[10,21−24] Nevertheless, they show completive power conversion efficiencies among their solution-processable small-molecule acceptor counterparts. A detailed study was dedicated to the effect of different groups at the core part of phthalic imide, resulting in a power conversion efficiency as high as 2.89%.[25−27] Having phthalic imide moieties connected to benzothiadiazole via a vinyl bridge, Bloking et al. showed that a power conversion efficiency of 2.54% is achievable with open circuit voltage as high as 0.96 V.[28] Compounds with a diimide structure are also investigated as potential photoluminescent materials. Photoluminescence (PL) properties of (poly)imides depend on their structure. The chromophores used define the color of emitted light. Changing the structure of

the compound allows emission in the range from blue to red to be obtained.[29] Sauve and co-workers[30] showed naphthalene imides with thiophene which emit red light with a quantum yield of 0.56. In our previous works we showed azomethine diimides emitting blue, green-blue, and green light.[31−34]

Recently, research efforts have been focused on the development of alternating compounds consisting of segments of different electron-donating/accepting (D/A) properties and resulting in a low band gap.[2,3,35−37] By selection of the donor and acceptor units, the compound architecture enables modification of the energy levels of the highest occupied molecular orbital (HOMO), lowest unoccupied molecular orbital (LUMO), energy gap, and charge transport ability.[37] Among various D−A conjugated systems, azomethine diimide-based compounds from small molecules and polymers constitute a promising family of materials whose properties can be explored in (opto)electronic devices. Azomethines due to the presence of an imine bond (−N=CH−) are isoelectronic to their carbon analogues, making them suitable alternatives to conventional conjugated materials.[38] One can find a detailed review article by Iwan and Sek[39] covering a wide range of azomethine and poly(azomethine) structures used in photovoltaic devices having power conversion efficiencies ranging between 0.0002% and 3.9%. Dingemans and co-workers[40] described liquid crystalline poly(azomethine)s as hole transport materials in solar cell devices and found a power conversion efficiency of 0.12%, the highest one obtained among other devices due to the presence of a thiophene moiety. A recent study was also conducted with azomethines with different substituents such as benzothiazole, thiophene, and bithiophene on their electrical and photovoltaic properties.[41−44] Moreover, PL properties of azomethines containing triphenyl-amine[39] or fluorene[45] have been investigated. Skene et al.[46] described thiophene−fluorene azomethines emitting blue, green, and red light with quantum yields of ca. 10%.

In this paper, the continuation of the effort in synthesis of new azomethine diimides along with polymers which form alternating electron-donating−electron-accepting systems is presented. The idea of preparation of compounds with both imine and diimide moieties was presented in our previous works.[31−34] The objective of this work was to synthesize new azomethine diimides end-capped with thiophene, bithiophene, and (ethylenedioxy)thiophene rings and polymers and study their chosen properties important from the point of view of their potential applications in organic optoelectronics. In the present paper we show a comprehensive study of the obtained compounds' physical properties, such as thermal (differential scanning calorimetry (DSC)), optical (UV−vis, PL), and electrochemical (cyclic voltammetry (CV), differential pulse voltammetry (DPV)), which were investigated and are discussed in relation to their chemical structure. The optical properties of the thin films were characterized using spectroscopic ellipsometry, and the complex dielectric function was obtained. Additionally, HOMO and LUMO levels and E_g were calculated theoretically using density functional theory (DFT). The synthesized compounds differ in the chemical structure of the diimide core, the kind of end-capping group, and the structure of the moieties between the diimide rings and imine linkages.

2. EXPERIMENTAL SECTION

2.1. Materials. Benzene-1,2,4,5-tetracarboxylic dianhydride (pyromellitic dianhydride, PMDA), 1,4,5,8-naphthalenetetra-

carboxylic dianhydride (NDTA), 2,3,5,6-tetramethyl-1,4-phenylenediamine, 1,4-naphthalenediimide, 2-thiophenecarboxaldehyde, 2,2′-bithiophene-5-carboxaldehyde, toluene-4-sulfonic acid (PTS), trifluoroacetic acid (TFA), N,N-dimethylacetamide (DMA), N,N-dimethylformamide (DMF), N-methyl-2-pyrrolidinone (NMP), chloroform, and pyridine were purchased from Aldrich Chemical Co. and used as received. N,N′-Bis(4-amino-2,3,5,6-tetramethylphenyl)naphthalene-1,4,5,8-dicarboximide (DANDI) was prepared according to a previously described procedure.[31] N,N′-Bis(4-amino-2,3,5,6-tetramethylphenyl)-phtalene-1,2,4,5-dicarboximide (DAPhDI) was prepared according to a previously described procedure.[34] Indium tin oxide (ITO) was purchased from Aldrich Chemical Co. The surface resistance of ITO was about 15−20 Ω/square. PEDOT:PSS (poly(3,4-(ethylenedioxy)thiophene):poly-(styrenesulfonate)) and P3HT (poly(3-hexylthiophene)) were also purchased from Aldrich Chemical Co.

2.2. Synthesis of Diamines and Dialdehydes. *2.2.1. N,N′-Bis(5-aminonaphthalenyl)naphthalene-1,4,5,8-dicarboximide (DANDI-2).* NTDA (3 mmol, 0.805 g), 1,4-naphthalenediamine (15 mmol, 2.3730 g), and imidazole (23.25 mmol, 1.5 g) were added to 30 mL of dry pyridine and refluxed under an argon atmosphere. After 6 h, the mixture was cooled to room temperature. The precipitating diamine was collected by filtration and washed with water and then with hot methanol. The resulting diamine was dried in vacuum. Yield: 65%, violet solid. ^{1}H NMR (DMSO-d_6, δ, ppm): 5.92 (s, NH$_2$, 4H), 6.73 (d, Ar H, 2H), 6.95 (dd, Ar H, 2H), 7.16 (t, Ar H, 2H), 7.75 (t, Ar H, 2H), 7.61 (t, Ar H, 2H), 8.27 (d, Ar H, 2H), 8.76 (s, 4H). FTIR (KBr, cm^{-1}): ν 3438, 3365 (−NH$_2$ stretch), 1708, 1673 (C=O imide stretch), 1630 (−NH$_2$ deformation), 1344 (C−N stretch), 769 (imide ring deformation). Anal. Calcd for C$_{34}$H$_{20}$N$_4$O$_4$ (548.55 g/mol): C, 74.45; H, 3.67; N, 10.21. Found: C, 74.08; H, 3.66; N, 10.28.

2.2.2. 3,4-(Ethylenedioxy)thiophene-2-carboxaldehyde (EDOT-CHO). A solution of 3,4-(ethylenedioxy)thiophene (1 g, 7.1 mmol) in dry Et$_2$O (15 mL) was cooled to −45 °C under an argon atmosphere and treated with 1.6 M n-BuLi (12 mL). The mixture was stirred for 45 min, DMF (2 mL, 25.2 mmol) was slowly added, and the solution was stirred for another 2.5 h. The mixture was allowed to warm to room temperature and hydrolyzed with aqueous HCl. The precipitated aldehyde was filtered, washed with water, and dried in vacuum. Yield: 90%. Mp: 142 °C. ^{1}H NMR (CDCl$_3$, δ, ppm): 9.91 (s, 1H), 6.79 (s, 1H), 4.36−4.34 (t, 2H, J = 3.3 Hz), 4.27−4.25 (t, 2H, J = 4.2 Hz). ^{13}C NMR (100 MHz, CDCl$_3$, δ, ppm): 178.9, 128.3, 128.0, 127.7, 109.9, 64.7, 63.9.

2.3. Synthesis of Azomethine Diimides. *2.3.1. Synthesis of Azomethine Phthalic Diimides (AzPhDIs).* Diamine DAPhDI (0.2553 g, 0.5 mmol), monoaldehyde 2-thiophene-carboxaldehyde (0.2286 g, 1 mmol), 2,2′-bithiophene-5-carboxaldehyde (0.1973 g, 1 mmol), or 3,4-)ethylenedioxy)-thiophene-2-carboxaldehyde (0.170 g; 1 mmol), and 0.2 mL of TFA were added to 3 mL of DMA and heated (160 °C) under an argon atmosphere. After 20 h the mixture was cooled to room temperature. The precipitate was collected by filtration, washed with methanol, and dried in vacuum. Yields of AzPhDIs: AzPhDI-1, 72%; AzPhDI-2, 80%; AzPhDI-3, 19%.

2.3.1.1. AzPhDI-1. ^{1}H NMR (CDCl$_3$, δ, ppm): 8.54 (s, H$_{Ar}$ [phenylene]), 8.26 (s, CH=N). FTIR (KBr, cm^{-1}): ν 1778, 1727 (C=O imide stretch), 1626 (CH=N), 1372 (C−N stretch), 731 (imide ring deformation).

2.3.1.2. AzPhDI-2. ^{1}H NMR (CDCl$_3$, δ, ppm): 8.55 (s, H$_{Ar}$ [phenylene]), 8.19 (s, CH=N). FTIR (KBr, cm^{-1}): ν 1774, 1727 (C=O imide stretch), 1615 (CH=N), 1371 (C−N stretch), 732 (imide ring deformation).

2.3.1.3. AzPhDI-3. ^{1}H NMR (CDCl$_3$, δ, ppm): 8.53 (s, H$_{Ar}$ [phenylene]), 8.24 (s, CH=N),. FTIR (KBr, cm^{-1}): ν 2923, 2872 (C−H aliphatic), 1776, 1724 (C=O imide stretch), 1618 (CH=N), 1371 (C−N stretch), 732 (imide ring deformation).

2.3.2. Synthesis of Azomethine Naphthalene Diimides (AzNDIs). Diamine DANDI (0.2803 g, 0.5 mmol) or DANDI-2 (0.5 mmol, 0.2743 g), monoaldehyde 2-thiophenecarboxaldehyde (0.2286 g, 1 mmol), 2,2′-bithiophene-5-carboxaldehyde (0.1973 g, 1 mmol), or 3,4-(ethylenedioxy)thiophene-2-carboxaldehyde (0.170 g, 1 mmol), and 0.2 mL TFA were added to 5 mL of DMA and heated (160 °C) under an argon atmosphere. After 16 h, this mixture was cooled to room temperature. Then the reaction mixture was poured into methanol, and the resulting precipitate was filtered off, extracted with boiling methanol (Soxhlet apparatus), and dried in vacuum. Yields of AzNDIs: AzNDI-1, 69%; AzNDI-2, 56%; AzNDI-3, 77%; AzNDI-4, 26%.

2.3.2.1. AzNDI-1. ^{1}H NMR (DMSO, δ, ppm): 8.95 (s, CH=N), 8.81 (s, H$_{Ar}$ [napthalene]). FTIR (KBr, cm^{-1}): ν 1715, 1677 (C=O imide stretch), 1611 (CH=N), 1341 (C−N stretch), 769 (imide ring deformation).

2.3.2.2. AzNDI-2. ^{1}H NMR (DMSO, δ, ppm): 8.93 (s, CH=N), 8.81 (s, H$_{Ar}$ [napthalene]). FTIR (KBr, cm^{-1}): ν 1714, 1676 (C=O imide stretch), 1607 (CH=N), 1341 (C−N stretch), 769 (imide ring deformation).

2.3.2.3. AzNDI-3. ^{1}H NMR (DMSO, δ, ppm): 8.80 (s, H$_{Ar}$ [napthalene]), 8.74 (s, CH=N). FTIR (KBr, cm^{-1}): ν 2921, 2868 (C−H aliphatic), 1714, 1674 (C=O imide stretch), 1626 (CH=N), 1339 (C−N stretch), 769 (imide ring deformation).

2.3.2.4. AzNDI-4. ^{1}H NMR (DMSO, δ, ppm): 8.81 (s, H$_{Ar}$ [napthalene]), 8.27 (s, CH=N). FTIR (KBr, cm^{-1}): ν 2924, 2873 (C−H aliphatic), 1712, 1675 (C=O imide stretch), 1621 (CH=N), 1334 (C−N stretch), 772 (imide ring deformation).

2.4. Synthesis of Poly(azomethine naphthalene imide)s (polyAzNDIs). Diamine DANDI-2 (0.5 mmol, 0.2743 g), dialdehyde 2,5-thiophenedicarboxaldehyde (0.0701 g, 0.5 mmol) or 2,2′-bithiophene-5,5′-dicarboxaldehyde (0.1111 g, 0.5 mmol), and a pinch of p-toluenesulfonic acid (PTS) were added to 5 mL of DMA and heated (160 °C) under an argon atmosphere. After 16 h, this mixture was cooled to room temperature. The precipitate was collected by filtration, extracted with boiling methanol (Soxhlet apparatus), and dried in vacuum. DANDI-2 condensed with 2,5-thiophenedicarboxaldehyde resulted in polymer polyAzNDI-1, while DANDI condensed with 2,2′-bithiophene-5,5′-dicarboxaldehyde gave polymer polyAzNDI-2. Yields of polymers: polyAzNDI-1, 80%, black solid; polyAzNDI-2, 60%, red solid.

2.4.1. PolyAzNDI-1. FTIR (KBr, cm^{-1}): ν 1711, 1667 (C=O imide stretch), 1613 (CH=N), 1340 (C−N stretch), 769 (imide ring deformation).

2.4.2. PolyAzNDI-2. FTIR (KBr, cm^{-1}): ν 1715, 1675 (C=O imide stretch), 1604 (CH=N), 1341 (C−N stretch), 768 (imide ring deformation).

2.5. Blend Preparation. Blends were prepared by dissolving the desired amount of studied compounds and PMMA in NMP to form a homogeneous solution (1% (v/v) concentration of the compound in PMMA). Films cast on glass were dried in a vacuum oven at 90 °C for 10 h.
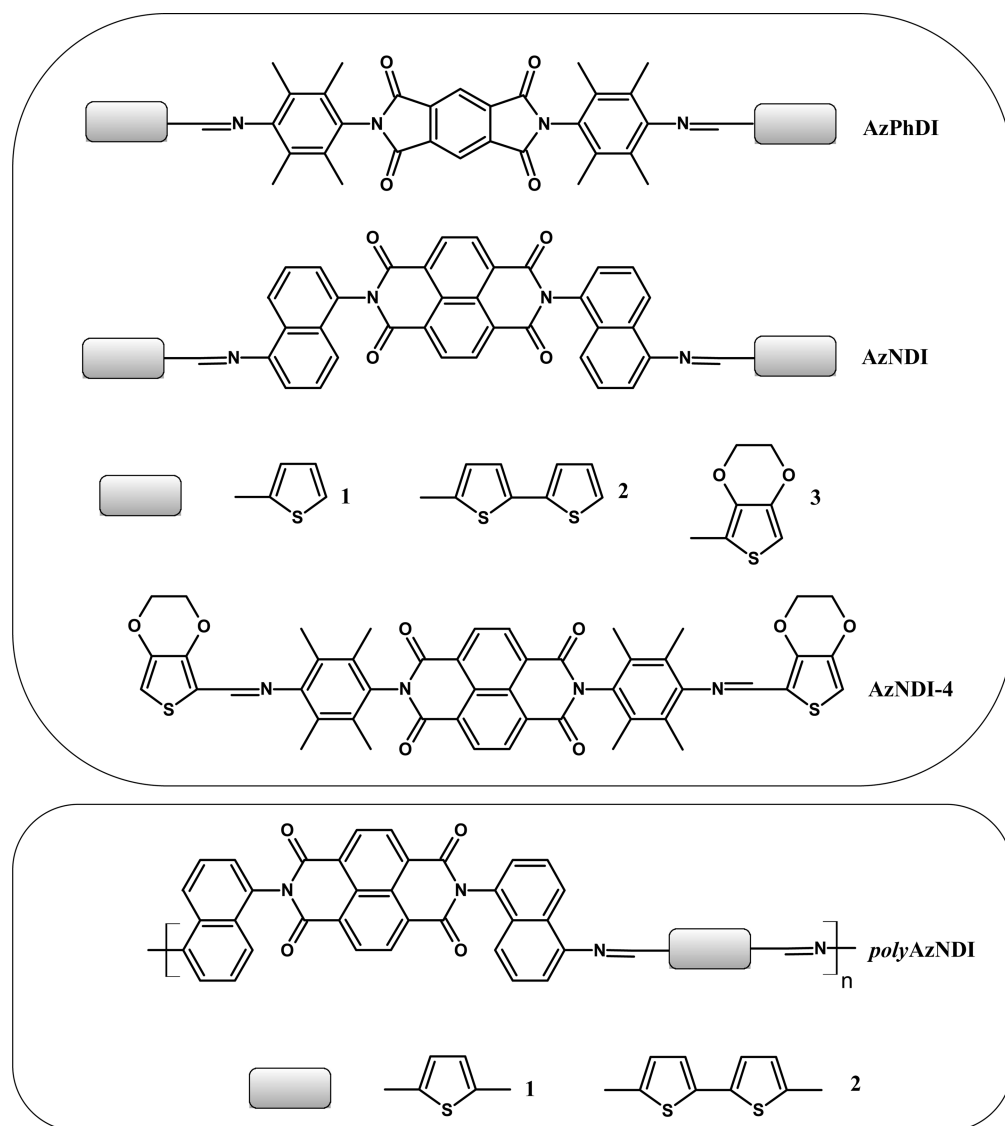
Figure 1. Chemical structures of synthesized azomethine diimides and poly(azomethine imide)s.

2.6. Measurements. Proton nuclear magnetic resonance (^{1}H NMR) spectra were recorded on a Bruker AC 400 MHz spectrometer using chloroform (CDCl$_3$) as the solvent and TMS as the internal standard. Infrared (IR) spectra were acquired on a PerkinElmer Spectrum One using KBr pellets. Elemental analyses were performed using a PerkinElmer Analyzer 2400. Thermogravimetric analysis (TGA) was done with a TGA/DSC1 Mettler-Toledo thermal analyzer with a heating rate of 10 °C/min in a stream of nitrogen (60 cm^3 min^{-1}). DSC was performed with a TA-DSC 2010 apparatus (TA Instruments, Newcastle, DE) under nitrogen using aluminum sample pans at a heating rate of 20 °C min^{-1}. UV–vis absorption spectra were recorded in solution using a PerkinElmer Lambda Bio 40 UV–vis spectrometer. Photoluminescence spectra were measured using a Varian Cary Eclipse spectrometer. Electrochemical measurements were carried out using an Eco Chemie Autolab PGSTAT128n potentiostat in the three-electrode configuration using a glassy carbon electrode, platinum coil, and silver wire as the working, auxiliary, and quasi reference electrodes, respectively. Potentials are referenced with respect to the ferrocene/ferrocenium (Fc/Fc$^+$) redox couple, which was used as the internal standard.

Cyclic and differential pulse voltammetry experiments were conducted in a standard one-compartment cell under an argon atmosphere. Bu$_4$NPF$_6$ (0.2 M) (Aldrich, 99%) dissolved in MeCN (Carlo Erba, HPLC grade) was used as the supporting electrolyte. The NIR–vis–UV ellipsometric characterization was done using a Woollam M-2000 rotating compensator ellipsometer, which spans an energy range from 0.73 to 6.5 eV. The ellipsometric measurements were performed at many different angles of incidence (45–75° in 5° sequences). The measured complex quantity $\rho = (\tan \psi)e^{i\Delta}$ can be converted to a complex pseudodielectric function $\langle \varepsilon(\omega) \rangle$ assuming that the multilayer can be described by a single and uniform dielectric layer using[46−49]

$$\langle \varepsilon_s \rangle = \varepsilon_a \left(\sin^2(\theta) + \sin^2(\theta) \tan^2(\theta) \frac{(1-\rho)^2}{(1+\rho)^2} \right) \tag{1}$$

where θ is the angle of incidence and ε_a the dielectric function of the ambient, for air taken to be 1. If the sample under study is just a single homogeneous material, then the pseudodielectric function is the same as the dielectric function, representing the correct material response. If the sample is not a single
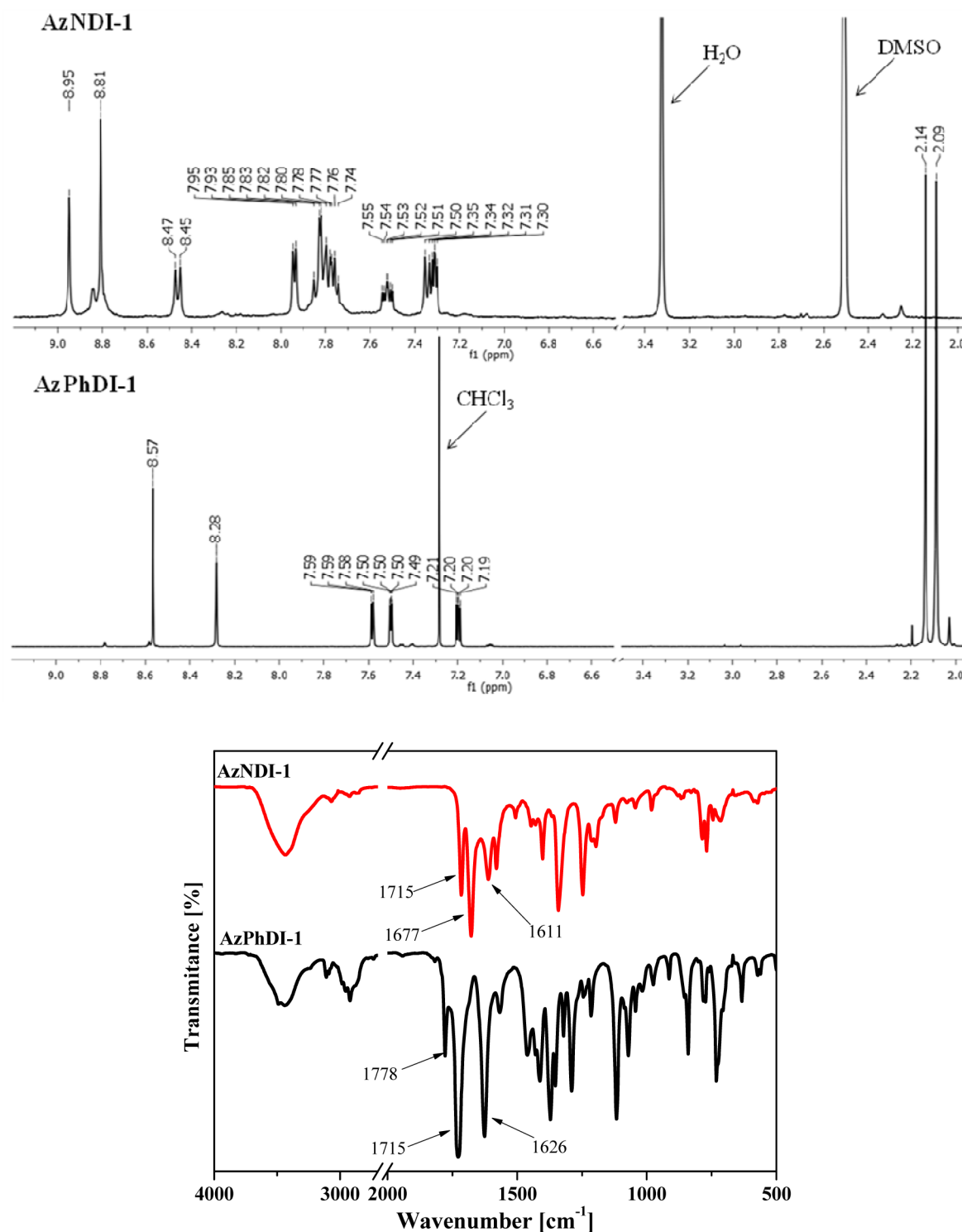
Figure 2. ^{1}H NMR and FTIR spectra of AzPhDI-1 and AzNDI-1.

homogeneous material, e.g., a thin layer on a substrate, eq 1 can be applied as well, assuming a single homogeneous substrate, but then the result is termed a "pseudodielectric function" and indicated by $\langle\varepsilon\rangle$. The dielectric function for the studied polymer films was then obtained by fitting the measured ellipsometric response, ψ and Δ, using a complex model dispersion relation. At first, fitting was performed for the angle of incidence 65°. For improving the sensitivity and accuracy, the fitting was cross-checked afterward at other angles (45–75°). The film thicknesses were determined by measuring the

layer thickness at four positions with a stylus DEKTAK profilometer before and after doping. The data were fitted using WVASE software with the known layer thickness, with the assumption of a negligible roughness, i.e., small compared to the wavelength, using a generic oscillator. As a result, a preliminary model for the real (ε_1) and imaginary (ε_2) parts of the dielectric function was obtained. Then the fitting was refined either by adding more oscillators or by a point to point fit and checking the Kramers–Kronig consistency. DFT calculations were carried out using the Gaussian09[50] package

and employing the hybrid B3LYP[51−53] exchange correlation potential combined with the 6-31G(d,p) basis set. Ground-state geometries (constrained to the C_2 symmetry point group) were fully optimized until a stable local minimum was found and was confirmed by normal-mode analysis (no imaginary frequencies were present). To improve numerical accuracy of the calculations (possible energy oscillations during SCF), two-electron integrals and their derivatives were calculated in a modified way employing the pruned (99 590) integration grid consisting of 99 radial shells and 590 angular points per shell. On these ground-state geometries, time-dependent density functional theory (TD-DFT)[54−60] calculations were performed to find the first 50 excited states employing the same level of theory. The energies and their corresponding oscillator strengths were retrieved using GaussSum 2.2.[61] Molecular orbital plots were generated from ".cube" files with Gabedit 2.4.6.[62]

2.7. Photovoltaic Cell Preparation. The regioregular P3HT as the polymer matrix was chosen. Photovoltaic cells were fabricated on ITO-covered glass slides (15 mm × 15 mm) which were cleaned in an ultrasonic bath using organic solvents. Next the ITO was covered with a PEDOT:PSS thin film by spin-coating and left for 30 min in a vacuum heater at 70 °C. After 30 min the active layer, that is, P3HT:AzPhDI dissolved in chloroform with weight ratio 1:1, was spun over the PEDOT:PSS thin film. At the end photovoltaic cells were defined by aluminum electrodes thermally evaporated in vacuum. Current−voltage (I−V) characteristics of the devices were measured using the Keithley 2400 sourcemeter. The device was illuminated with a maximum intensity of 1.3 mW/cm².

3. RESULTS AND DISCUSSION

In this paper, the continuation of efforts in the synthesis of materials for potential optoelectronic applications and the new low molecular compounds and polymers bearing imine linkages, diimide units, and thiophene rings is presented. Additionally, the chosen properties of the synthesized compounds presented in this paper are compared with those of their analogues, which have been described in our previous work.[33]

3.1. Synthesis and Characterization. The new azomethine diimides were prepared from diamine-containing five- or six-membered diimide units, i.e., DAPhDI,[34] DANDI,[31] and the new DANDI-2. The diamine DANDI-2 was prepared from condensation reaction of excess 1,4-naphthalenediamine with 1,4,5,8-naphthalenetetracarboxylic dianhydride (NTDA). The diamines DAPhDI and DANDI-2 were applied for condensation with three aldehydes, i.e., 2-thiophenecarboxaldehyde, 2,2′-bithiophene-5-carboxaldehyde, and 3,4-(ethylenedioxy)-thiophene-2-carboxaldehyde. DANDI was utilized for reaction with 3,4-(ethylenedioxy)thiophene-2-carboxaldehyde. Thus, azomethine diimides end-capped with thiophene, bithiophene, and (ethylenedioxy)thiophene units were prepared. The poly(azomethine imide)s were synthesized from DANDI-2 and 2,5-thiophenedicarboxaldehyde or 2,2′-bithiophene-5,5′-dicarboxaldehyde. These compounds form a block of electron-accepting (A) and electron-donating (D) systems along the polymer. The chemical structures of the obtained compounds are presented in Figure 1.

In our previous paper we have reported azomethine diimides obtained from DANDI and 2-thiophenecarboxaldehyde or 2,2′-bithiophene-5-carboxaldehyde and the corresponding poly-

mers.[33] Thus, the properties of the prepared azomethine diimides can be compared from three points of view: (i) the chemical structure of the diimide core, (ii) the type of end-capped group of the compounds, and (iii) the structure of the moieties between the diimide rings and imine linkages.

The assigned chemical structures of all synthesized compounds were identified through the data from ¹H NMR and FTIR spectroscopy measurements. Their expected chemical constitution was confirmed by FTIR studies. Exemplary ¹H NMR and FTIR spectra of AzPhDI-1 and AzNDI-1 are presented in Figure 2.

The absence of the residual amino (−NH₂) and aldehyde (−CHO) groups together with the appearance of a band typical for imine bonds (HC═N−) was confirmed by FTIR and NMR spectra. In FTIR spectra of the investigated compounds, in each case the characteristic band for the HC═N− stretching vibration was detected in the spectral range of 1604−1626 cm⁻¹ (cf. section 2). The exact position of this band in the investigated compounds varies by up to 22 cm⁻¹ and is shifted toward lower wavenumbers for the azomethine diimides end-capped with bithiophene rings (AzPhDI-2, AzNDI-2) and also the polymer with such units (poly(AzNDI-2). The wavenumber of these compounds is lower than that for the others, which means that the length of the imine bond in AzPhDI-1, AzPhDI-3, AzNDI-1, AzNDI-3, and poly(AzNDI-1) is larger than in AzPhDI-2, AzNDI-2, and poly(AzNDI-2). The lower wavenumber of the imine group absorption indicates the better conjugation of π-electrons with phenyl ring π-electrons caused by the influence of the bithiophene unit. Compounds with a phthalic diimide core containing thiophene and bithiophene rings exhibited a higher frequency of the analyzed band in comparison with azomethine naphthalenediimides, which proves that the largest decrease of the conjugation takes place. The possible explanation of this effect can be that the π-electrons in the double bond are less involved in conjugation. In the case of AzNDI-1 and AzNDI-2 compounds obtained from DANDI described in our previous work, there was a lack of influence of the number of thiophene rings on the wavenumber of the imine bond, which was at 1626 and 1620 cm⁻¹ in low molecular compounds and polymers, respectively.[33] When comparing the influence of the structure of the moieties between the diimide rings and imine linkages, the better conjugation is exhibited in the compounds with additional naphthalene units (AzNDI-1 and AzNDI-2) than in corresponding azomethine diimides with a tetramethyl-substituted phenyl ring between the imide and azomethine bond.[33] In the ¹H NMR spectra of azomethine diimides, a singlet signal due to the hydrogen atom present in the imine unit and multiplets of the protons in the aromatic rings were found. A shift of the position of the imine group signal, depending on the chemical structure, was observed. The protons of HC═N− appeared in the range of 8.19−8.95 ppm (cf. section 2).

The solubility of the synthesized compounds was qualitatively determined by the dissolution of 2.5 mg of the studied materials in 1 mL of different organic solvents at room temperature and under heating. The solubility data of the azomethine diimides and poly(azomethine imide)s in different organic solvents are listed in Table 1.

AzNDIs were found to be more soluble in strong polar solvents than their five-membered analogues AzPhDIs. Comparing the solubility of AzNDIs with that of the corresponding compounds described in our previous work,[33]

Table 1. Solubility Behavior of the Investigated Azomethine Diimides and Polymers[a]

compd	NMP	DMSO	THF	CHCl₃	CH₂Cl₂	cyclohexanone
AzPhDI-1	+	+	±	++	±	+
AzPhDI-2	±	+	±	+	±	+
AzPhDI-3	+	++	+	++	++	+
AzNDI-1	++	++	±	++	++	++
AzNDI-2	++	++	±	±	±	±
AzNDI-3	++	+	−	±	−	−
AzNDI-4	+	±	±	+	±	±
polyAzNDI-1	±	±	±	±	±	±
polyAzNDI-2	±	±	±	±	±	±

[a]The qualitative solubility was tested with a 2.5 mg sample in 1 mL of solvent: (++) soluble at room temperature, (+) soluble after heating, (±) partially soluble after heating, (−) not soluble.

it was found that replacement of the tetramethylphenyl rings with naphthalene units improves their solubility in NMP and DSMO.

3.2. Thermal Properties. It was found that forming stable, amorphous glassy states at/or above room temperature is desirable for hole/electron transport materials.[63] The gradual growth of crystallites of hole/electron transport materials induced by the Joule heat can induce phase separation. This results in detachment at the interfaces of the electrode/transport layer and deterioration, which are themselves thought to be important degradation factors, and then failure of stability and durability.[63] Thus, a lot of attention is paid to organic low molar mass compounds that readily form glasses above room temperature. On the other hand, when the voltage is applied and current is flowing through organic devices, Joule heating processes arise.[63] Thus, temperature stability is required. DSC and TGA in a nitrogen atmosphere were applied to examine the thermal properties of the obtained azomethine diimides and polymers.

3.2.1. DSC Investigations. Formation of the glassy state in synthesized azomethine diimides was investigated by DSC. A strong correlation between the thermal properties of the compounds and their chemical structures has been found. Thus, different behaviors of azomethine diimides during DSC heating and cooling runs were observed. The first and second run heating scans of the investigated compounds were carried out with a heating rate of 20 °C/min. The second heating was recorded immediately after rapid cooling. Figure S1 in the Supporting Information presents the DSC thermograms of exemplary azomethine diimides—AzPhDI-1, AzPhDI-2, and AzNDI-1. The first run heating scan showed glass transition temperatures (T_g) for compounds AzNDI-2 and AzNDI-4 at 291 and 192 °C, respectively. The results are similar to those obtained for azomethine naphthalenediimides with thiophene (T_g = 195 °C) and bithiophene (T_g = 174 °C) moieties prepared also from DANDI and described in our previous work.[33] For end-capped compounds with thiophene (AzPhDI-1 and AzNDI-1) and (ethylenedioxy)thiophene (AzPhDI-3) moieties, the first heating scan revealed both T_g values (AzPhDI-1, T_g = 215 °C; AzNDI-1, T_g = 280 °C; AzPhDI-3, T_g = 231 °C) and an endotherm indicating melting of the sample (AzPhDI-1, T_m = 403 °C; AzNDI-1, T_m = 377 °C; AzPhDI-3, T_m = 363 °C). On the other hand, the DSC curve of Az-NDI-3 did not show any transitions. During the second heating, all samples exhibited only the glass transition (except

for AzNDI-2, which exhibited both T_g and T_m). These temperatures are collected in Table 2.

Table 2. Thermal Properties of the Studied Compounds

compd	T_5[a] (°C)	T_{10}[a] (°C)	T_{max}[b] (°C)	CR[c] (%)	T_g (°C)
AzPhDI-1	418	427	419, 453	50	217
AzPhDI-2	399	409	403, 462	46	176
AzPhDI-3	376	389	386, 457	48	241
AzNDI-1	413	472	406, 565	55	277
AzNDI-2	390	472	409, 540	59	291
AzNDI-3	404	487	408, 553	62	278
AzNDI-4	345	392	414, 554	45	191
polyAzNDI-1	362	495	381, 555	58	190
polyAzNDI-2	468	483	485, 554	52	130

[a]T_5 and T_{10} are temperatures at 5% and 10% weight loss, respectively. [b]Temperature of maximum decomposition rate. [c]Residual weight when heated to 800 °C in nitrogen.

Thus, all obtained azomethine diimides are molecular glasses. In the DSC thermogram of AzPhDI-2 during the second heating run, apart from the glass transition, "cold" crystallization (exothermic peak) at 242 °C and a melting endotherm at 325 °C were detected (cf. Figure S1b in the Supporting Information). Comparing AzPhDIs with azomethine naphthalenediimides described in our previous work[33] and AzNDI-4 and considering the diimide structure, compounds with a phthalic diimide unit as the core exhibited higher T_g values. The influence of the end-capped group on T_g was found to be different for AzPhDIs than for AzNDIs. Introduction of naphthalene units between the diimide structure and imine linkages (AzNDI-3) caused an increase of T_g in relation to AzNDI-4 containing tetramethylphenyl moieties. The compound with naphthalenediimide containing bithiophene rings (AzNDI-2) exhibited the highest T_g, contrary to the compound with a phthalic diimide core (AzPhDI-2), which showed the lowest T_g.

3.2.2. Thermal Stability. TGA analyses were utilized to examine the thermal stability of the obtained azomethine naphthalenediimides and polymers. The registered thermograms of AzPhDI-2 and the corresponding AzNDI-2 are given in Figure 3 as examples.

Analysis of the TGA curves allowed estimation of the mass loss associated with the processes of degradation up to 800 °C, and the temperature of the maximum decomposition rate (T_{max}) is evidenced by the differential thermogravimetric (DTG) curve. The TGA curves of all compounds indicate the existence of two reaction stages, reflected in two peaks in the differential weight loss curve (DTG). Only in the case of AzNDI-2, AzNDI-3, and poly(AzNDI-1) are the two observed degradation steps separated. In this case the first step is connected with a mass loss of around 6% and the second with an about 20% mass loss. The thermal stability of the compounds which were evaluated in terms of 5% and 10% weight loss (T_5, T_{10}), T_{max}, and residual weight at the end of the experiment are listed in Table 2. Compounds with a naphthalenediimide core exhibited higher T_{10}, T_{max}, and residual weights at 800 °C compared to azomethine diimides with a five-membered imide ring. All compounds exhibited high thermal stability, with the value of T_5 in the range 345−468 °C, and an excellent residual weight at 800 °C within the range of 46−62%.
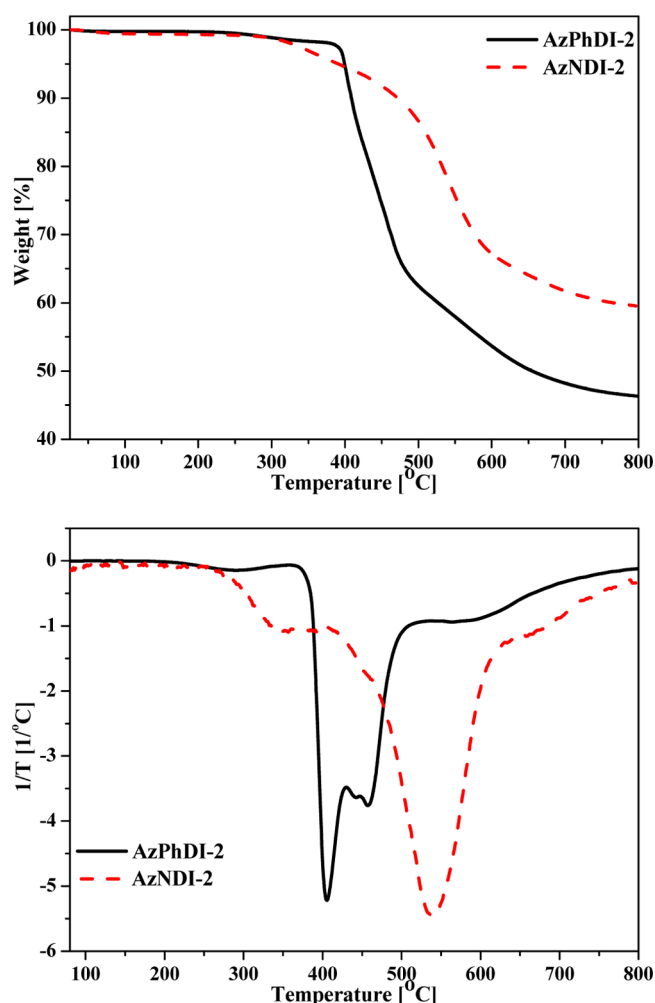
Figure 3. TGA and DTG curves of AzNPhDI-2 and AzNDI-2.

3.3. Photophysical Properties. The photophysical properties such as absorption and emission in the UV−vis range of the studied azomethine naphthalenediimides and poly(azomethine imide)s were analyzed by UV−vis absorption and photoluminescence (PL) spectroscopies in NMP and chloroform solutions and in the solid state as blends with poly(methyl methacrylate) (PMMA). PMMA has wide applications as an inert solid matrix for various spectroscopic and optoelectronic investigations for applications in OLEDs,[64−66] solar cells,[67,68] and organic switching devices.[69]

3.3.1. Ultraviolet−Visible Investigations. Absorbance spectra of azomethine diimides and polymers dissolved in NMP are depicted in Figure 4. Measurements were performed within the optical range from 260 to 550 nm. The data from absorption spectra of all studied compounds are summarized in Table S1 in the Supporting Information.

Electronic absorption spectra of the studied azomethine phthalic diimides showed similar characteristics, i.e., one main absorbance band. However, in the case of AzPhDI-1 and AzPhDI-3 a shoulder around 350 nm was seen. Both the position and the intensity of the absorption bands depend on the chemical structure of the compound. The position of the absorption maximum (λ_{max}) of compounds end-capped with bithiophenes was significantly shifted to lower energies as compared to that of other compounds with phthalic diimide rings. This confirms better conjugation in this compound as
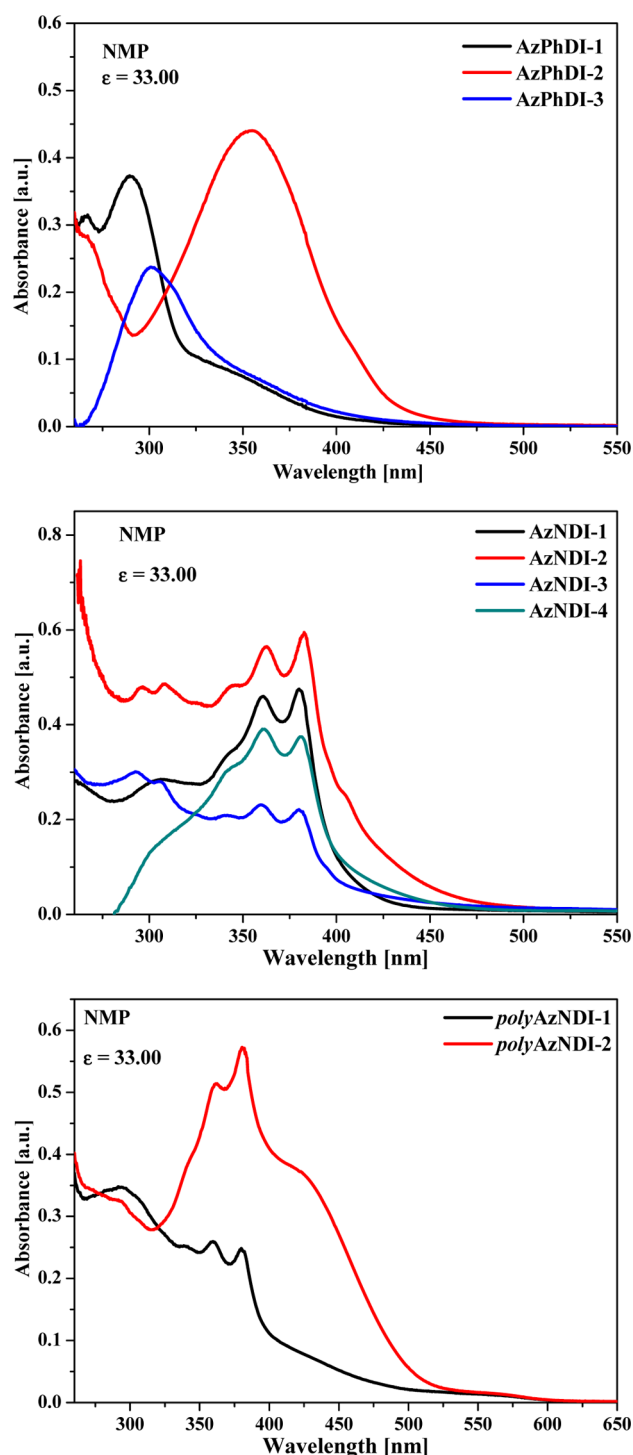

Figure 4. Absorption spectra of the studied compounds in NMP solution.

was concluded from FTIR and NMR data. In the UV−vis spectra electronic transitions of azomethine naphthalenediimides and polymers are dominated by a strong band of pronounced vibrational structure with three maxima at about 340, 360, and 380 nm, ascribed to the π−π* transition in the naphthalenediimide core.[33,70] Similarly, as was observed in AzPhDIs, the compounds with bithiophene rings exhibited an absorption range bathochromically shifted as compared to that of other materials (cf. Figure 4b,c). Despite the different polarities of the applied solvents, the spectra showed a λ_{max}

13077

dx.doi.org/10.1021/jp501168b | *J. Phys. Chem. C* 2014, 118, 13070−13086

position at almost the same wavelength (cf. Table S1, Supporting Information). Therefore, the solvatochromic effect was not observed in the studied compounds, an observation similar to that in the azomethine naphthalenediimides described in our previous works.[31−34] In the solid state, as blends with PMMA, the investigated compounds showed one main absorption band, which was in most cases hypsochromically shifted, along with a change from the solution state to the solid state.

3.3.2. Spectroscopic Ellipsometry. To determine the optical properties of thin films prepared using compounds containing phthahlic diimides (AzPhDI-1, AzPhDI-2, and AzPhDI-3) and naphthalenediimides (AzNDI-1, AzNDI-2, AzNDI-3, and AzNDI-4), spectroscopic ellipsometry was applied. For each compound the complex dielectric function ($\varepsilon_1 + i\varepsilon_2$) and complex refractive index ($n + ik$) were determined. The plots of both functions are presented in the Supporting Information. Here information about the absorption coefficient (α) is shown. Usually for material dissolved in solution, Beer's law is used for determination of α ($\alpha = 4\pi\kappa/\lambda_0$). However, for the thin film, where the layer thickness is much below the coherence length, the Fabry−Perrot interference fringes modify the spectrum. The absorption coefficient is described as[46,49]

$$\alpha(\omega) = \frac{\varepsilon_2(\omega)\omega}{cn(\omega)} \tag{2}$$

where ε_2 is the imaginary part of the dielectric function, n is the refractive index of the material, ω is the frequency, and c is the speed of light in vacuum. Using the above equation, absorption coefficients of the studied materials were calculated, and the resulting curves are presented in Figure S2 in the Supporting Information. For all three compounds a significant absorption above 3.5 eV from a phthalic diimide can be observed. Below 3.5 eV a different shape of the curves, due to the different end-capped group attached, can be noticed. Interestingly, the value of the absorption coefficient for AzPhDI-2 is 2 times stronger than those measured for AzPhDI-1 and AzPhDI-3. The reason is a higher conjugation of the end-capped group (bithiophene) which should result in better planarization of the molecule. This also results in better overlapping of the π orbitals, which also results in a much higher absorption coefficient of the phthalic group in this molecule. These results are in full agreement with the results of UV−vis spectroscopy measured for dissolved materials and with FTIR and NMR characteristics. As in the case of the compounds containing phthalic diimides, use of the naphthalenedimiides and different end-capping groups strongly influences the absorption coefficient spectra. For compounds containing thiophene and bithiophene (AzNDI-1 and AzNDI-2, respectively), the absorption coefficients are much higher than for those containing 3,4-(ethylenedioxy)thiophene end-capping groups.

The data from spectroscopic ellipsometry can also be compared with the results of TD-DFT calculations in terms of allowed transitions within this group of compounds. The results of these calculations are gathered in Table S2 in the Supporting Information.

What is no doubt worth noting is the fact that, in each case, the HOMO−LUMO transition is not allowed, possibly due to symmetry-related selection rules (oscillator strength equal to 0). Moreover, within the first 50 excited states, there are only several cases with significant, nonzero oscillator strength, therefore simplifying the assignment. In the case of pyromelitic

derivatives (AzPhDI-1−3), the first allowed transitions are due to excitations from phenylene/thiophene → thiophene (AzPhDI-1) and π−π* transitions on bithiophene (AzPhDI-2) and EDOT (AzPhDI-3). The relative energy of these transitions corresponds well with structural diversity. In the case of bithiophene, it is highly red-shifted due to a higher conjugation. The higher energy side of the spectra correspond to the rest of the transitions. For AzPhDI-1, it covers π−π* transitions on the pyromelitic core (29) on the thiophene moiety (34, 45) and some minor contribution from charge transfer transitions from thiophene to the core and vice versa (33, 49, respectively). For AzPhDI-2 the higher energy transitions are dominated by π−π* excitations on bithiophene and the core (12, 15). In case of AzPhDI-3, the situation is very much the same with π−π* transitions on the EDOT moiety (26) and the core (36, 38). The remaining NDI derivatives follow a similar pattern; however, the contribution from the naphthalene units is much more pronounced. In AzNDI-1 the first allowed transition is mainly a naphthalene → thiophene π−π* excitation, but the situation changes when moving to highly conjugated species such as AzNDI-2 and AzNDI-3, where the first allowed transitions are located on bithiophene and EDOT, respectively. The most unifying characteristic however between NDI-based derivatives is the common contribution of the NDI-located π−π* transitions to the spectrum, which is more pronounced in the case of AzNDI-4 due to the lack of naphthalene units. These transitions also carry a substantial oscillator strength and give rise to a vibrational structure. A comparison of normalized ellipsometric curves with oscillator strengths from TD-DFT calculations for AzPhDI-3 and AzNDI-1 is presented in Figure 5 (for a full comparison, see the Supporting Information). It can be clearly seen that in terms of allowed electronic transitions the results match the experimental data. In the case of pyromelitic derivatives, the long shoulder on the low-energy side corresponds to the transitions on the end-capped units (thiophene, bithiophene, and EDOT). For the rest of the molecules, the situation is slightly more complicated. From DFT study it seems that the lower lying allowed excited states carry a contribution from the end caps, but the shape of the experimental curve is very similar and may result mainly from the NDI-centered excitations of a superposition of NDI, naphthalene (phenylene), and thiophene moieties.

3.3.3. Photoluminescence Properties. The emission spectra were recorded with different excitation wavelengths (λ_{ex}) in NMP and chloroform solutions as well as in the solid state as blends with nonemissive PMMA. The influence of the excitation wavelength on the PL properties, the position of the emission band maximum (λ_{em}) and the intensity of emitted light, is presented in Figure 6. The emission spectral data of the studied compounds are summarized in Table S3 in the Supporting Information.

All the compounds with naphthalenediimides in the structure (except AzNDI-3) exhibited a very week emission in chloroform solution, and thus, these results are not discussed in this paper. In the PL spectrum of AzNDI-1, a broad emission band with two maxima at an excitation of 340 nm is seen (cf. Figure 6b). The investigated compounds in solution at different excitation wavelengths exhibited a single emission band. Compounds containing azomethine phthalic diimides emitted light with lower intensity in CHCl₃ compared to NMP except the compound end-capped with an (ethylenedioxy)thiophene unit (AzPhDI-3). Taking into account the intensity of emitted
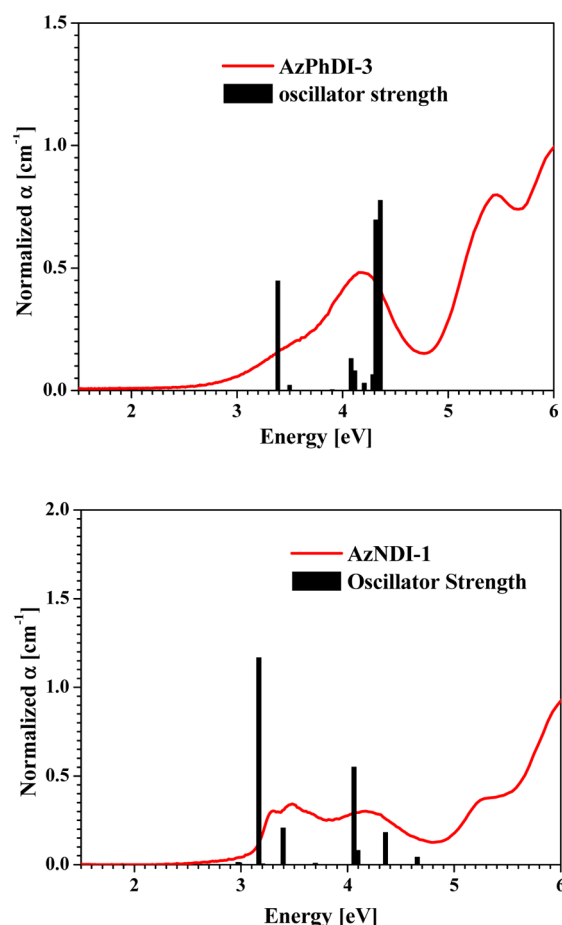
Figure 5. Major contributing oscillator strengths and normalized ellipsometric curves of AzPhDI-3 and AzNDI-1.

light in the same solution concentration, photoluminescence of azomethine phthalic diimides AzPhDI-1 and AzPhDI-2 was significantly more intense than that of the corresponding azomethine naphthalenediimides AzNDI-1 and AzNDI-2. The intensity of light emission of AzPhDIs decreases in the following order: AzPhDI-1 > AzPhDI-3 > AzPhDI-2. A significant effect of bithiophene end groups on the decrease of the PL intensity was revealed. The emission wavelength of the azomethine diimides and polyAzNDI-1 in solutions was independent of λ_{ex}, except for compounds with a bithiophene ring (AzPhDI-2, AzNDI-2, and polyAzNDI-2) and AzNDI-3. For those compounds, together with an increase of λ_{ex}, a bathochromic shift in the λ_{em} position was observed in the PL spectra. All studied compounds emitted blue light, an observation similar to that for azomethine diimides and polymers with a tetramethylphthalic ring between the diimide structure and imine linkages reported in our previous work.[33] All azomethine diimides and polymers emitted light with the highest intensity at λ_{ex} = 360 nm, except for AzNDI-2 and Az-NDI-3 (cf. Table S3, Supporting Information). Considering the effect of the solvent polarity on the PL spectra, in all cases of compounds with a phthalic diimide unit, a hypsochromic shift of λ_{em} was found with a decrease in solvent polarity; thus, they exhibited solvatochromic behavior. Such behavior may be evidence of the photoinduced intramolecular charge-transfer character of the excited state in these compounds.[71,72]

It should be noticed that the UV−vis absorption spectra of the investigated compounds overlap slightly with their emission spectra. The emission maxima are strongly red-shifted from their optical absorption maxima (cf. Figure 6c). The Stokes shifts, which are important from a practical point of view of potential applications, were in the range of 5885−16356 cm^{-1}.

Additionally, the fluorescence characteristics of the obtained compounds in the solid state as blends with PMMA were studied. The normalized PL spectra of the blends excited with a wavelength corresponding to the highest emission intensity in NMP solution are presented in Figure 6d. The PL spectra of the compounds in the blends changed, compared with their spectra in NMP solution. In comparison with that of the solution, λ_{em} of the blends was hypsochromically shifted in the range of 4−40 nm; however, all blends emitted blue light (cf. Figure 6e). The highest differences between λ_{em} values of compounds in blends and NMP solution were detected in the case of AzNDIs.

3.4. Electrochemical Properties. The suitability of the use of compounds in a given electronic application can be determined by their redox properties, which are frequently investigated by electrochemical methods. In this study, the redox properties of the studied compounds were investigated using CV and DPV. The obtained electrochemical data are presented in Table S4 in the Supporting Information, whereas the CV and DPV voltammograms of azomethine diimides and polymers are collected in Figure 7.

All measurements were carried out on a glassy carbon electrode (the working electrode). For polyAzNDI-2, in comparison the platinum electrode was used, allowing recording of up to five separated reduction peaks, which was not possible on a platinum wire electrode. In addition, the reductions peaks were much less visible on the Pt electrode. Furthermore, Red$_3$ was almost invisible on the Pt wire. It is expected that at lower potentials platinum becomes a hard Lewis acid in nature. Probably a stable adduct with the reduced form of C=O is formed (interaction between Pt and a hard O$^-$ anion). This prevents further flow of the charge.

For each azomethine diimide a fully reversible reduction process toward the formation of an anion radical according to the mechanism proposed by Hsiao et al.[73] was recorded. Compounds consisting of a phthalic diimide structure (AzPhDIs) revealed almost identical properties during the reductions (cf. Figure 7a). In each case three, fully reversible reduction steps were measured (peak-to-peak separation ~60 mV). This clearly shows that the thiophene ring modifications do not affect the position of the LUMO. There is no resonance contact of these fragments with the diimide moiety. All of the investigated compounds possess electropolymerizable units as end groups. Possibly, these may have undergone the polymerization process during oxidation, such as for compounds consisting of thiophenes and azomethine double bonds.[74] However, in this case, polymerization did not occur. The oxidation potentials (within the range from 0.3 to 0.53 V) are also too low to be assigned to the oxidations of the thiophene ring. The decomposition of the compound occurs faster than polymerization of thiophene units. The similarity of the properties during the reduction can also be observed in the case of a series of compounds with a naphthalenediimide unit (AzNDIs). First, they are easier to reduce than phthalic diimide analogues—at a potential slightly below −0.7 V. This is another example of the common phenomenon that the anion is better stabilized on a naphthalenediimide than phthalic diimide moiety and therefore is more easily formed. All of the naphthalenediimide Red$_2$ values are also similar for all discussed
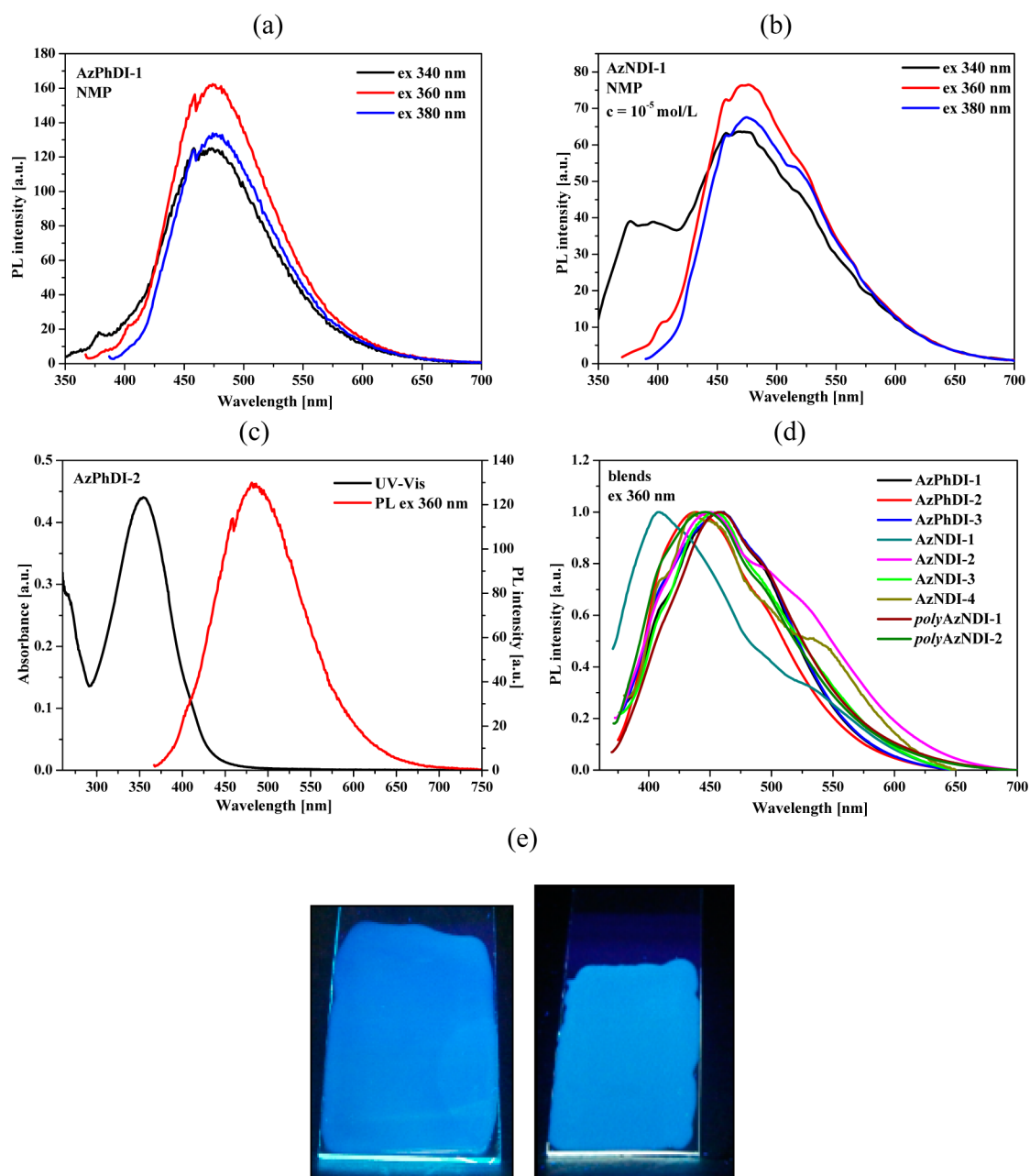
Figure 6. (a, b) Fluorescence spectra of (a) AzPhDI-1 and (b) AzNDI-1 in NMP, (c) PL and UV−vis spectra of AzPHDI-2 in NMP, (d) PL spectra of all compounds in the blend, and (e) photographs of AzPhDI-2 (left) and polyAzNDI-1 (right) in blends irradiated with light at 366 nm.

derivatives, i.e., in the range from −1.13 to −1.30 V. Potentials Red$_3$ and Red$_4$ are also almost alike. The reduction processes are fully reversible (peak-to-peak separation ∼60 mV) (cf. Figure 7). A graphical comparison of polymers with the corresponding model compounds under electrochemical measurements is shown in Figure 7c,d. As one can see, there is almost no change in the voltammograms of polyAzNDI-2 and its model compound AzNDI-2. This means that the polymerization does not affect the redox properties of AzNDI-2. Therefore, any differences in the properties in the solid state are a consequence of different intermolecular interactions (not intramolecular). On the other hand, for AzNDI-1 and its polymeric analogue (polyAzNDI-1), a significant oxidation potential shift (to the lower potential) as a consequence of polymerization was observed. Importantly, in this case there is also a reduction potential shift. Quite unexpectedly, it was more

difficult for diimide units in the polymer to undergo reduction than those in AzNDI-1 (Figure 7d). Moreover, in both cases, the recorded peaks are slightly less apparent—probably due to sterical difficulties in the flow of charge between a polymeric molecule and the surface of the electrode.

From the onset oxidation and reduction potentials in the CV and DPV voltammograms, the energies of the HOMO and LUMO levels (or rather ionization potentials (IPs) and electron affinities) can be readily estimated, assuming the IP of ferrocene to be equal to −4.8 eV, according to well-established equations.[75] The calculated HOMO and LUMO levels together with the electrochemical energy band gap (E_g) are presented in Table 3.

The experimental CV data are well correlated with the DPV data. Considering the influence of the compound structure on the LUMO energy level and E_g, it was observed that variation of
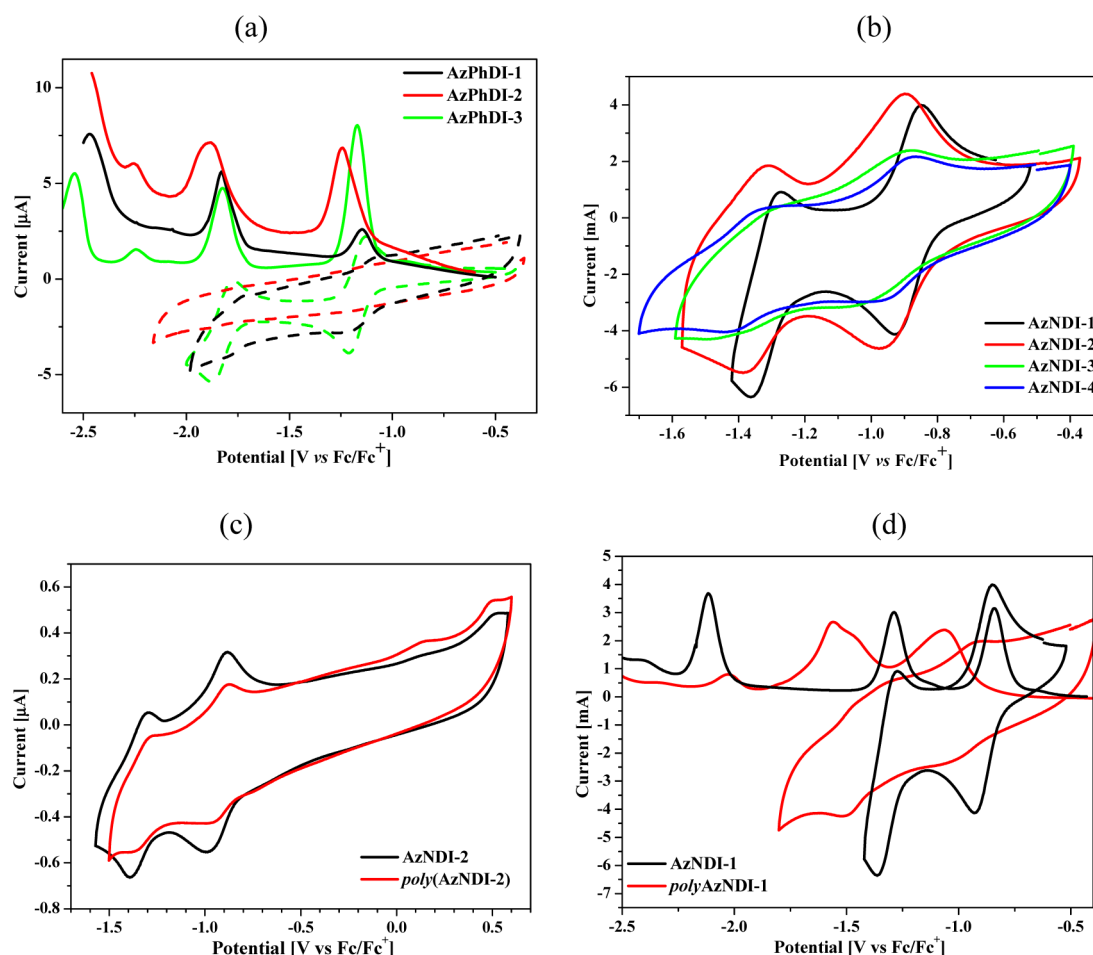
Figure 7. CV (dashed lines) and DPV (solid lines) voltammograms of AzPhDIs (a), CV voltammograms of AzNDIs (b), CV voltammograms of polyAzNDI-2 and AzNDI-2 (c), and CV and DPV curves of polyAzNDI-1 and AzNDI-1 (d). The measurements were performed in acetonitrile containing 0.1 M nBu_4NPF_6 using a GC working electrode and referenced against the $Cp_2Fe^{+/0}$ couple (for CV a scan rate of 100 mV/s was used).

Table 3. Comparison of the HOMO/LUMO Energy Levels and Band-Gap Energies Determined by Electrochemistry Measurement and DFT Calculation[a]

	CV			DPV			DFT		
code	E_{HOMO} (V)	E_{LUMO} (V)	E_g (eV)	E_{HOMO} (V)	E_{LUMO} (V)	E_g (eV)	E_{HOMO} (V)	E_{LUMO} (V)	E_g (eV)
AzPhDI-1	−5.27	−3.72	1.55	−5.22	−3.77	1.45	−5.85	−2.95	2.89
AzPhDI-2	−5.12	−3.74	1.38	−5.09	−3.73	1.36	−5.61	−2.94	2.66
AzPhDI-3	−5.35	−3.77	1.58	−5.31	−3.77	1.54	−5.65	−2.86	2.79
AzNDI-1	−5.89	−4.00	1.89	−5.79	−4.09	1.70	−5.58	−3.26	2.31
AzNDI-2	−5.22	−3.97	1.25	−5.22	−4.01	1.21	−5.41	−3.25	2.15
AzNDI-3	−5.26	−3.96	1.40	−5.27	−4.00	1.27	−5.37	−3.18	2.20
AzNDI-4	−5.26	−3.93	1.33	−5.25	−4.03	1.22	−5.57	−3.13	2.45
polyAzNDI-1	−5.22	−3.92	1.30	−5.20	−3.93	1.27			
polyAzNDI-2	−5.17	−3.95	1.22	−5.16	−4.02	1.14			

[a] $E_{HOMO} = -4.82 - E_{ox,onset}$. $E_{LUMO} = -4.82 - E_{red,onset}$. $E_g = E_{ox,onset} - E_{red,onset} = E_{HOMO} - E_{LUMO}$.

the end groups of the diimide core can be used to tune the HOMO energy and consequently the band gap of the material while leaving the LUMO practically intact. The values of E_g of the azomethine diimides were the lowest for compounds end-capped with bithiophene units, an observation similar to that for azomethine diimides described in our former paper.[33] The effect of the diimide structure on E_g was studied, and it was found that compounds with a six-membered diimide unit exhibited a lower electrochemical energy gap in relation to AzPhDIs. Polymers exhibited a lower E_g as compared to their

model compounds. Summarizing, all of the studied compounds reveal very good properties during reduction (multiple steps and fully reversible), and they are promising electron-transporting materials.

3.5. DFT Calculations. To investigate the electron density distribution, a set of DFT calculations were carried out. The geometries were fully optimized on the presented level of theory in vacuum and then further analyzed. The theoretically calculated HOMO and LUMO energy levels and E_g are presented in Table 3, whereas the HOMO and LUMO
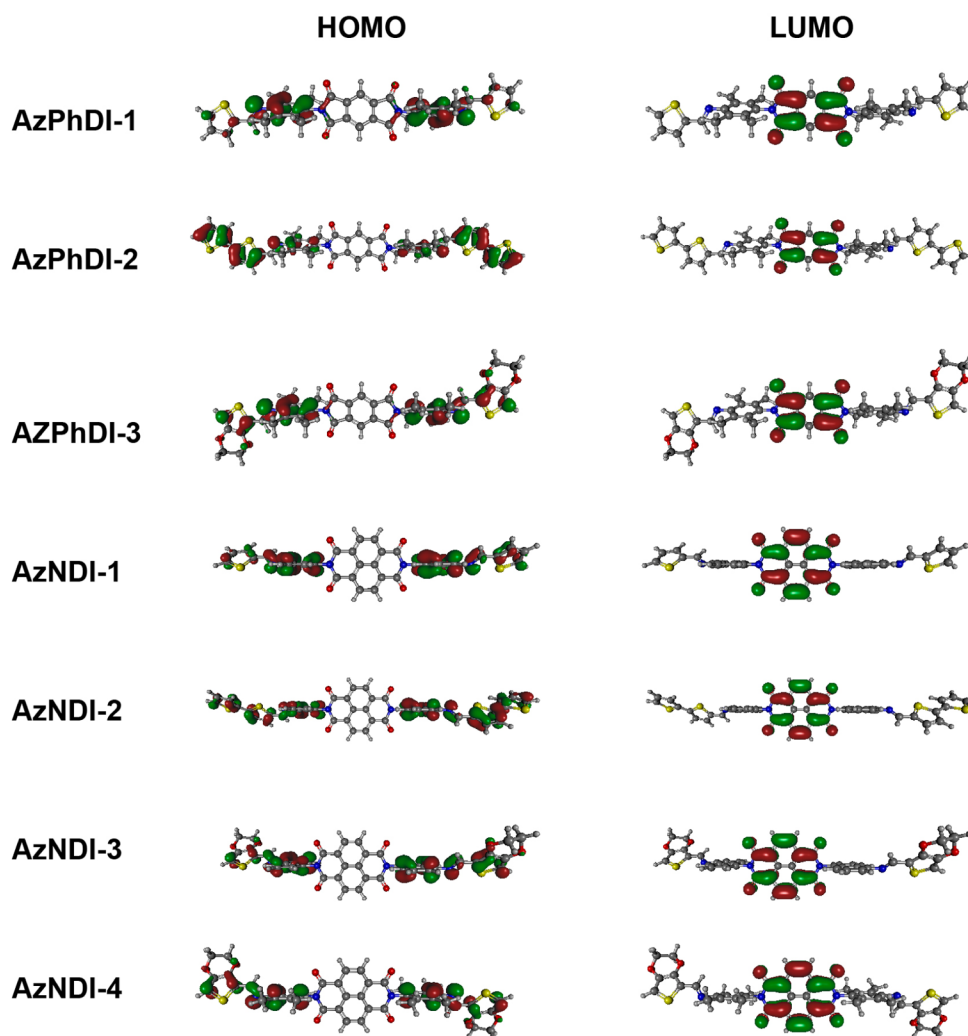
Figure 8. HOMO and LUMO contours of the obtained azomethine diimides.

contours of the investigated azomethine diimides are shown in Figure 8.

The HOMO and LUMO orbitals in each case are exclusively space-separated in almost the same part of the molecule. The localization of the LUMO on the strongly electron-accepting diimide core is a key characteristic in this class of compounds and is also pronounced in this study. On the other hand, in the case of the HOMO some minor differences may be found within the studied molecules. In AzPhDI-1 and AzNDI-1 the contribution from the thiophene moiety to the HOMO is small, and therefore, it is located almost exclusively on the tetramethylphenyl and naphthalene moieties, respectively. Incorporation of EDOT instead of thiophene with strongly electron-donating −OCHH$_2$CH$_2$O− groups (AzPhDI-3, AzNDI-3, AzNDI-4) induces a higher contribution of this moiety to the HOMO. Finally, exchanging thiophene with bithiophene results in spreading of the HOMO almost evenly along the naphthalene and bithiophene in AzNDI-2 and the dominant participation of bithiophene in the HOMO in AzPhDI-2. Another important fact is the analysis of the HOMO/LUMO energy levels and their corresponding E_g values. According to Table 3, the HOMO level varies from −5.37 eV for AzNDI-3 and AzNDI-4 to −5.85 eV for AzPhDI-1. Systematic comparison reveals that the exchange of thiophene for (ethylenedioxy)tiophene or bithiophene is followed by a rise in the HOMO level by 0.2 eV (AzPhDI-1 and AzNDI-1) and at the same time lowering of the E_g value. The exchange of the diimide core also affects the HOMO level with a drop in energy by 0.2 eV when moving from six-membered naphthalenediimide to five-membered pyrromellitic diimide. As for the changes in LUMO energies, there is virtually no affect of the side aromatic azomethines on the LUMO of a specific compound. On the other hand, there is a great dependence on the type of diimide that is used. Six-membered rings cause a drop in the LUMO level by 0.3 eV and therefore a drop in E_g as well. By combining these two effects of interplay between the electron-donating character of the azomethine substituent and the size of the aromatic core, one can easily change the value of E_g from 2.15 eV (for AzNDI-2) to 2.89 eV (for AzPhDI-1). The comparison of the theoretically predicted HOMO/LUMO values with the experimental data reveals significant differences. These problems may be interpreted in terms of the functional formulation and the effects that lie inside. First, there may be some unfortunate miscalculations due to the sum of several errors which usually cancel each other. Second, the differences may be a result of the dynamics of the electrochemistry. The flow of charge also affects the molecule; therefore, it is sometimes better to think of the measured values in terms of ionization potential and electron affinity. Nevertheless, despite the differences in values, the

theoretically calculated values follow the pattern of the electrochemical data. The LUMO levels for AzNDI derivatives are 0.3 eV smaller than for AzPhDIs. At the same time the drops and rises in the HOMO are directly correlated to the experimental data. The differences in E_g are a direct consequence of these phenomena and the reasons mentioned above.

3.6. Characterization of Photovoltaic Cells. Preliminary investigations of obtained model compounds AzPhDI-1 and AzPhDI-2 as active layers in solar cells were carried out. The fabricated devices have the following architecture: ITO/PEDOT:PSS/P3HT:AzPhDI/Al. The aluminum electrode acts as the cathode (collecting electrons), while ITO is applied as the anode for the purpose of collecting holes. The regioregular P3HT with a HOMO level of about −4.8 eV and LUMO level of about -2.7 eV was applied as the donor in the photovoltaic devices. PEDOT:PSS was used in the devices as an anode buffer layer. The active layer consists of P3HT and AzPhDI (weight ratio 1:1). Two types of heterojunctions, with thicker (208 nm) and thinner (150 nm) active layers, were fabricated. For the prepared devices the parameters characterizing the photovoltaic effect were measured. The samples were illuminated with a light source with a power of 1.3 mW/cm^2, and measurements were made using a Keithley 2400 source with a picoamperemeter. From the obtained characteristics of photocurrent density−voltage, the current density J_{sc}, open-circuit voltage V_{OC}, and fill factor (FF) and conversion efficiency η defined as

$$FF = \frac{I_m V_m}{I_{SC} V_{OC}}$$

$$\eta = \frac{I_{SC} V_{OC} FF}{P_{light}}$$

were calculated (P_{light} is the input optical power). We also determined the maximum power of the cell P_{max} (μW). The obtained $I-V$ curves in the dark and under illumination are presented in Figure 9, and the corresponding photovoltaic performances are summarized in Table 4.

Taking into account the photovoltaic parameter, which depends on the chemical structure of the active layer, which determines the HOMO level of the donor and LUMO level of the acceptor and UV−vis properties, that is, the open-circuit voltage (V_{OC}), it can be seen that the device comprising P3HT with azomethine phthalic diimide end-capped with thiophene rings showed significantly lower V_{OC}. It should be stressed that the device with AzPhDI containing bithiophene units exhibited a much higher value of V_{OC} above 1 V. Considering the conversion efficiency, the effect of the chemical structure is less pronounced. It was found that the thickness of the active layer influences the maximal power point and power conversion efficiency. For thinner layers, we have found higher maximum power values and higher power conversion efficiency.

4. CONCLUSIONS

New compounds consisting of a phthalic diimide or naphthalenediimide core end-capped with thiophene, bithiophene, and (ethylenedioxy)thiophene units were synthesized. The structure of the resulting compounds was checked using ^{1}HNMR and FTIR spectra, showing the appearance of characteristic signals from typical bonds. FTIR also revealed better conjugation of compounds containing bithiophene.
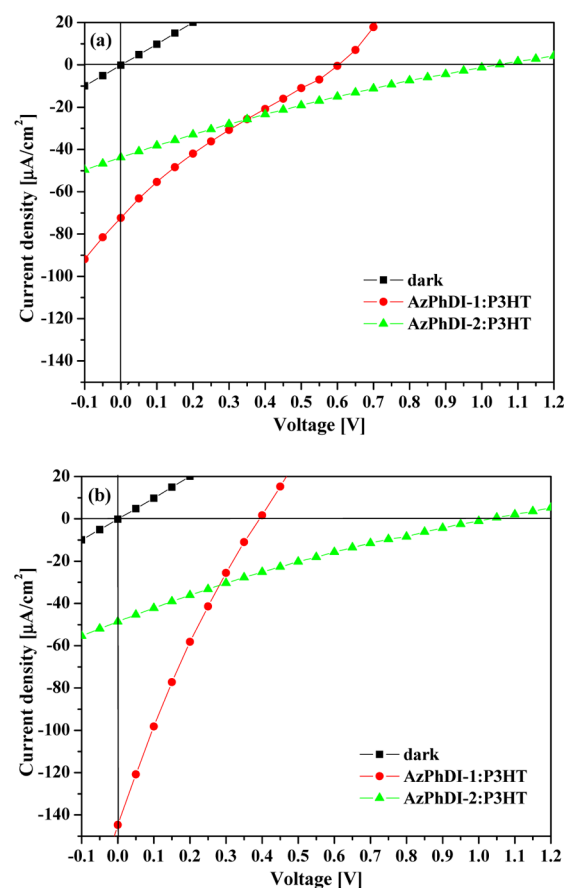

Figure 9. $J-V$ characteristics of organic photovoltaic cells: (a) ITO/PEDOT:PSS/active layer/AL (active layer thickness 208 nm), (b) ITO/PEDOT:PSS/active layer/AL (active layer thickness 150 nm).

Table 4. Characteristics of Devices in the Configuration ITO/PEDOT:PSS/Active Layer (P3HT:AZPhDI Weight Ratio 1:1)/Al under Light Illumination (1.3 mW/cm^2)

active layer	J_{SC} (μA/cm^2)	V_{OC}(V)	FF	η (%)	P_{max} (μW)
AzPhDI-1:P3HT, thickness 208 nm	67.12	0.60	0.23	0.69	9.14
AzPhDI-2:P3HT, thickness 208 nm	43.24	1.04	0.21	0.73	9.56
AzPhDI-1:P3HT, thickness 150 nm	144.45	0.39	0.21	0.90	11.81
AzPhDI-2:P3HT, thickness 150 nm	48.60	1.03	0.20	0.78	10.22

Thermal properties were determined using differential scanning calorimetry, while thermal stability was determined using thermogravimetric and differential thermogravimetric techniques. All small molecules exhibited properties characteristic of molecular glasses. In the second heating run only glass transition temperatures between 176 and 291 °C were found. The compounds have adequate thermal stability for applications in optoelectronic devices (T_5 in the range between 345 and 468 °C). To determine photophysical properties, the UV−vis and photoluminescence spectroscopic studies were performed in both solution (in NMP and chloroform) and the solid state (in blends with PMMA). All compounds emitted blue light. The dielectric function was determined for each compound using spectroscopic ellipsometry. The resulting absorption coefficients revealed a strong correlation with the

chemical structure of the presented polymers. This behavior was additionally correlated with that obtained using DFT calculations. Finally, the electrochemical properties of the studied compounds were characterized using cyclic voltammetry and differential pulse voltammetry. All compounds show a fully reversible reduction peak. The position of the peaks was strongly correlated with the chemical structure. The energy gap obtained from the CV measurement differed between 1.22 and 1.89 eV and for each compound was slightly bigger (by a maximum of 0.19 eV) than those obtained from the DPV measurement. However, the difference between the experimentally obtained E_g and that predicted from the DFT calculations was much bigger (more than 1 eV). The strong difference between theoretical and experimental data is because DFT calculates E_g from the molecular orbitals, while CV measures the ionization energy. The preliminary photovoltaic experiments (device architecture ITO/PEDOT:PSS/active layer/Al) suggested that model compounds end-capped with bithiophene units are better for photovoltaic applications. The obtained results showed that the chemical structure of the organic compound and thickness of the active layer in the device influence the photovoltaic properties of organic solar cells. The conversion efficiency of the fabricated devices was in the range of 0.69−0.90%. The high value of V_{OC} (above 1 V) was obtained for an active layer consisting of azomethine phthalic diimide with bithiophene rings.

ASSOCIATED CONTENT

Ⓢ Supporting Information

DSC thermograms, UV−vis absorption characterization, photoluminescence, spectroscopic ellipsometry, TD-DFT calculations, and electrochemical data. This material is available free of charge via the Internet at http://pubs.acs.org

AUTHOR INFORMATION

Corresponding Author
*Phone: +48 323591642. E-mail: ewa.schab-balcerzak@us.edu.pl.

Notes
The authors declare no competing financial interest.

ACKNOWLEDGMENTS

REFERENCES

(1) Pron, A.; Reghu, R. R.; Rybakiewicz, R.; Cybulski, H.; Djurado, D.; Grazulevicius, J. V.; Zagorska, M.; Kulszewicz-Bajer, I.; Verilhac, J.-M. Triarylamine Substituted Arylene Bisimides as Solution Processable Organic Semiconductors for Field Effect Transistors. Effect of Substituent Position on Their Spectroscopic, Electrochemical, Structural, and Electrical Transport Properties. *J. Phys. Chem. C* **2011**, *115*, 15008−15017.

(2) Bujak, P.; Kulszewicz-Bajer, I.; Zagorska, M.; Maurel, V.; Wielgus, I.; Pron, A. Polymers for electronics and spintronics. *Chem. Soc. Rev.* **2013**, *42*, 8895−8999.

(3) Lincker, F.; Heinrich, B.; De Bettignies, R.; Rannou, P.; Pécaut, J.; Grévin, B.; Pron, A.; Donnio, B.; Demadrille, R. Fluorenone core donor−acceptor−donor π-conjugated molecules end-capped with dendritic oligo(thiophene)s: synthesis, liquid crystalline behaviour, and photovoltaic applications. *J. Mater. Chem.* **2011**, *21*, 5238−5247.

(4) Xu, Q.; Wang, J.; Chen, S.; Li, W.; Wang, H. Synthesis and characterization of naphthalene diimide polymers based on donor-acceptor system for polymer solar cells. *Express Polym. Lett.* **2013**, *7*, 842−851.

(5) Shirota, Y. Organic materials for electronic and optoelectronic devices. *J. Mater. Chem.* **2000**, *10*, 1−25.

(6) Shirota, Y. Photo- and electroactive amorphous molecular materials-molecular design, syntheses, reactions, properties, and applications. *J. Mater. Chem.* **2005**, *15*, 75−93.

(7) Plate, A.; Palato, S.; Lebel, O.; Soldera, A. Functionalization of molecular glasses: effect on the glass transition temperature. *J. Mater. Chem. C* **2013**, *1*, 1037−1042.

(8) Bakken, N.; Torres, J. M.; Li, J.; Vogt, B. D. Thickness dependent modulus of vacuum deposited organic molecular glasses for organic electronics applications. *Soft Matter* **2011**, *7*, 7269−7273.

(9) Dong, H.; Zhu, H.; Meng, Qi.; Gong, X.; Hu, W. Organic photoresponse materials and devices. *Chem. Soc. Rev.* **2012**, *41*, 1754−1808.

(10) Hu, Ch.; Zhang, Q. Synthesis and characterization of pyromellitic diimides-containing conjugated polymers. *Polym. Bull.* **2012**, *69*, 63−69.

(11) Qu, H.; Luo, J.; Zhang, X.; Chi, Ch. Dicarboxylic imide-substituted poly(*p*-phenylene vinylenes) with high electron affinity. *J. Polym. Sci., Part A: Polym. Chem.* **2010**, *48*, 186−194.

(12) Bhosale, Sh. V.; Jani, Ch. H.; Langford, S. J. Chemistry of naphthalene diimides. *Chem. Soc. Rev.* **2008**, *37*, 331−342.

(13) Gawrys, P.; Boudinet, D.; Zagorska, M.; Djurado, D.; Verilhac, J.-M.; Horowitz, G.; Pecaud, J.; Pouget, S.; Pron, A. Solution processible naphthalene and perylene bisimides: Synthesis, electrochemical characterization and application to organic field effect transistors (OFETs) fabrication. *Synth. Met.* **2009**, *159*, 1478−1485.

(14) Eftaiha, A. F.; Sun, J.-P.; Hill, I. G.; Welch, G. C. Recent advances of non-fullerene, small molecular acceptors for solution processed bulk heterojunction solar cells. *J. Mater. Chem. A* **2014**, *2*, 1201−1213.

(15) Lin, Y.; Li, Y.; Zhan, X. Small molecule semiconductors for high-efficiency organic photovoltaics. *Chem. Soc. Rev.* **2012**, *41*, 4245−4272.

(16) Segura, J. L.; Herrera, H.; Bauerle, P. Oligothiophene-functionalized naphthalimides and perylene imides: design, synthesis and applications. *J. Mater. Chem.* **2012**, *22*, 8717−8733.

(17) Fernando, R.; Mao, Z.; Muller, E.; Ruan, F.; Sauve, G. Tuning the Organic Solar Cell Performance of Acceptor 2,6-Dialkylamino-naphthalene Diimides by Varying a Linker between the Imide Nitrogen and a Thiophene Group. *J. Phys. Chem. C* **2014**, *118*, 3433−3442.

(18) Ren, G.; Ahmed, E.; Jenekhe, S. A. Non-Fullerene Acceptor-Based Bulk Heterojunction Polymer Solar Cells: Engineering the Nanomorphology via Processing Additives. *Adv. Energy Mater.* **2011**, *1*, 946−953.

(19) Sharenko, A.; Proctor, C. M.; van der Poll, T. S.; Henson, Z. B.; Nguyen, T.-Q.; Bazan, G. C. A High-Performing Solution-Processed Small Molecule: Perylene Diimide Bulk Heterojunction Solar Cell. *Adv. Mater.* **2013**, *25*, 4403−4406.

(20) Zhang, X.; Lu, Z.; Ye, L.; Zhan, C.; Hou, J.; Zhang, S.; Jiang, B.; Zhao, Y.; Huang, J.; Zhang, S.; et al. A Potential Perylene Diimide Dimer-Based Acceptor Material for Highly Efficient Solution-Processed Non-Fullerene Organic Solar Cells with 4.03% Efficiency. *Adv. Mater.* **2013**, *25*, 5791−5797.

(21) Zheng, Q.; Huang, J.; Sarjeant, A.; Katz, H. E. Pyromellitic Diimides: Minimal Cores for High Mobility n-Channel Transistor Semiconductors. *J. Am. Chem. Soc.* **2008**, *130*, 14410−14411.

(22) Wang, Z.; Kim, C.; Facchetti, A.; Marks, T. J. Anthracenedicarboximides as Air-Stable N-Channel Semiconductors for Thin-Film Transistors with Remarkable Current On−Off Ratios. *J. Am. Chem. Soc.* **2007**, *129*, 13362−13363.

(23) Dingemans, T. J.; Picken, S. J.; Murthy, N. S.; Mark, P.; StClair, T. L.; Samulski, E. T. Wholly Aromatic Ether-imides. Potential Materials for n-Type Semiconductors. *Chem. Mater.* **2004**, *16*, 966−974.

(24) Carroll, J. B.; Gray, M.; McMenimen, K. A.; Hamilton, D. G.; Rotello, V. M. Redox Modulation of Benzene Triimides and Diimides via Noncovalent Interactions. *Org. Lett.* **2003**, *5*, 3177−3180.

(25) Ding, L.; Ying, H.-Z.; Zhou, Y.; Lei, T.; Pei, J. Polycyclic Imide Derivatives: Synthesis and Effective Tuning of Lowest Unoccupied Molecular Orbital Levels through Molecular Engineering. *Org. Lett.* **2010**, *12*, 5522−5525.

(26) Zhou, Y.; Ding, L.; Shi, K.; Dai, Y.-Z.; Ai, N.; Wang, J.; Pei, J. A Non-Fullerene Small Molecule as Efficient Electron Acceptor in Organic Bulk Heterojunction Solar Cells. *Adv. Mater.* **2012**, *24*, 957−961.

(27) Zhou, Y.; Dai, Y.-Z.; Zheng, Y.-Q.; Wang, X.-Y.; Wang, J.-Y.; Pei, J. Non-Fullerene Acceptors Containing Fluoranthene-Fused Imides for Solution-Processed Inverted Organic Solar Cells. *Chem. Commun.* **2013**, *49*, 5802−5804.

(28) Bloking, J. T.; Han, X.; Higgs, A. T.; Kastrop, J. P.; Pandey, L.; Norton, J. E.; Risko, C.; Chen, C. E.; Bredas, J.; McGehee, M. D.; Sellinger, A. Solution-Processed Organic Solar Cells with Power Conversion Efficiencies of 2.5% using Benzothiadiazole/Imide-Based Acceptors. *Chem. Mater.* **2011**, *23*, 5484−5490.

(29) Liaw, D.-J.; Wang, K.-L.; Huang, Y.-C.; Lee, K.-R.; Lai, J.-Y.; Ha, C.-S. Advanced Polyimide Materials: Syntheses, Physical Properties and Applications. *Prog. Polym. Sci.* **2012**, *37*, 907−974.

(30) Fernando, R.; Mao, Z.; Sauvé, G. Rod-like Oligomers Incorporating 2,6-Dialkylamino Core-Substituted Naphthalene Diimide as Acceptors for Organic Photovoltaic. *Org. Electron.* **2013**, *14*, 1683−1692.

(31) Schab-Balcerzak, E.; Iwan, A.; Krompiec, M.; Siwy, M.; Tapa, D.; Sikora, A.; Palewicz, M. New Thermotropic Azomethine−naphthalene Diimides for Optoelectronic Applications. *Synth. Met.* **2010**, *160*, 2208−2218.

(32) Schab-Balcerzak, E.; Grucela-Zajac, M.; Krompiec, M.; Janeczek, H.; Siwy, M.; Sek, D. New Naphthalene Diimide-Based Compounds Containing Triarylamine Units and Imine Linkages: Thermal, Optical and Electrochemical Properties. *Synth. Met.* **2011**, *161*, 2268−2279.

(33) Schab-Balcerzak, E.; Grucela-Zajac, M.; Krompiec, M.; Niestroj, A.; Janeczek, H. New Low Band Gap Compounds Comprised of Naphthalene Diimide and Imine Units. *Synth. Met.* **2012**, *162*, 543−553.

(34) Bijak, K.; Grucela-Zajac, M.; Janeczek, H.; Wiacek, M.; Schab-Balcerzak, E. New Azomethine-Phthalic Diimides: Synthesis and Thermal, Optical and Electrochemical Characterization. *Synth. Met.* **2013**, *175*, 146−154.

(35) Kim, D. Y.; Cho, H. N.; Kim, C. Y. Blue light emitting polymers. *Prog. Polym. Sci.* **2000**, *25*, 1089−1139.

(36) Wei, Zh.; Xi, H.; Dong, H.; Wang, L.; Xu, W.; Hu, W.; Zhu, D. Blending induced stack-ordering and performance improvement in a solution-processed n-type organic field-effect transistor. *J. Mater. Chem.* **2010**, *20*, 1203−1207.

(37) Shi, Sh.; Xie, X.; Jiang, P.; Chen, S.; Wang, L.; Wang, M.; Wang, H.; Li, X.; Yu, G.; Li, Y. Naphtho[1,2-b:5,6-b′]dithiophene-Based Donor−Acceptor Copolymer Semiconductors for High-Mobility Field-Effect Transistors and Efficient Polymer Solar Cells. *Macromolecules* **2013**, *46*, 3358−3366.

(38) Iwan, A.; Sek, D. Processible polyazomethines and polyketanils: From aerospace to light-emitting diodes and other advanced applications. *Prog. Polym. Sci.* **2008**, *33*, 289−345.

(39) Iwan, A.; Sek, D. Polymers with triphenylamine units: Photonic and electroactive materials. *Prog. Polym. Sci.* **2011**, *36*, 1277−1325.

(40) Hindson, J. C.; Ulgut, B.; Friend, R. H.; Greenham, N. C.; Norder, B.; Kotlewski, A.; Dingemans, T. J. All-aromatic liquid crystal triphenylamine-based poly(azomethine)s as hole transport materials for opto-electronic applications. *J. Mater. Chem.* **2010**, *20*, 937−944.

(41) Iwan, A.; Boharewicz, B.; Tazbir, I.; Sikora, A.; Schab-Balcerzak, E.; Grucela-Zajac, M.; Skorka, L. Structural and electrical properties of mixture based on P3HT:PCBM and low band gap naphthalene diimide-imines. *Synth. Met.* **2014**, *189*, 183−192.

(42) Iwan, A.; Tazbir, I.; Sibiński, M.; Boharewicz, B.; Pasciak, G.; Schab-Balcerzak, E. Optical, Electrical and Mechanical Properties of Indium Tin Oxide on Polyethylene Terephthalate Substrates: Application in Bulk-Heterojunction Polymer Solar Cells. *Mater. Sci. Semicond. Process.* **2014**, *24*, 110−116.

(43) Iwan, A.; Schab-Balcerzak, E.; Korona, K. P.; Grankowska, S.; Kamińska, M. Investigation of Optical and Electrical Properties of New Aromatic Polyazomethine with Thiophene and Cardo Moieties toward Application in Organic Solar Cells. *Synth. Met.* **2013**, *185−186*, 17−24.

(44) Iwan, A.; Palewicz, M.; Krompiec, M.; Grucela-Zajac, M.; Schab-Balcerzak, E.; Sikora, A. Synthesis, Materials Characterization and Opto(electrical) Properties of Unsymmetrical Azomethines with Benzothiazole Core. *Spectrochim. Acta, A* **2012**, *97*, 546−555.

(45) Barik, S.; Bletzacker, T.; Skene, W. G. Π-Conjugated Fluorescent Azomethine Copolymers: Opto-Electronic, Halochromic, and Doping Properties. *Macromolecules* **2012**, *45*, 1165−1173.

(46) Yu, P. Y.; Cardona, M. *Fundamentals of Semiconductors: Physics and Materials Properties*, 4th ed.; Springer: Berlin, 2010.

(47) Azzam, R. M. A.; Bashara, N. M. *Ellipsometry and Polarized Light*; North Holland: Amsterdam, 1987.

(48) Gasiorowski, J.; Menon, R.; Hingerl, K.; Dachev, M.; Sariciftci, N. S. Surface morphology, optical properties and conductivity changes of poly(3,4-ethylenedioxythiophene): poly(styrenesulfonate) by using additives. *Thin Solid Films* **2013**, *536*, 211−215.

(49) Gasiorowski, J.; Hingerl, K.; Menon, R.; Plach, T.; Neugebauer, H.; Wiesauer, K.; Yumusak, C.; Sariciftci, N. S. Dielectric Function of Undoped and Doped Poly[2-methoxy-5-(3′,7′-dimethyloctyloxy)-1,4-phenylene-vinylene] by Ellipsometry in a Wide Spectral Range. *J. Phys. Chem. C* **2013**, *117*, 22010−22016.

(50) Frisch, M. J.; Trucks, G. W.; Schlegel, H. B.; et al. *Gaussian 09*, revision A.1; Gaussian, Inc.: Wallingford, CT, 2010.

(51) Becke, A. D. A new mixing of Hartree−Fock and local density-functional theories. *J. Chem. Phys.* **1993**, *98*, 1372−1377.

(52) Becke, A. D. Density-functional thermochemistry. III. The role of exact exchange. *J. Chem. Phys.* **1993**, *98*, 5648−5652.

(53) Lee, C. T.; Yang, W. T.; Parr, R. G. Development of the Colle-Salvetti correlation-energy formula into a functional of the electron density. *Phys. Rev. B* **1988**, *37*, 785−789.

(54) Bauernschmitt, R.; Ahlrichs, R. Treatment of electronic excitations within the adiabatic approximation of time dependent density functional theory. *Chem. Phys. Lett.* **1996**, *256*, 454−464.

(55) Casida, M. E.; Jamorski, C.; Casida, K. C.; Salahub, D. R. Molecular excitation energies to high-lying bound states from time-dependent density-functional response theory: Characterization and correction of the time-dependent local density approximation ionization threshold. *J. Chem. Phys.* **1998**, *108*, 4439−4449.

(56) Stratmann, R. E.; Scuseria, G. E.; Frisch, M. J. An efficient implementation of time-dependent density-functional theory for the calculation of excitation energies of large molecules. *J. Chem. Phys.* **1998**, *109*, 8218−8224.

(57) Van Caillie, C.; Amos, R. D. Geometric derivatives of excitation energies using SCF and DFT. *Chem. Phys. Lett.* **1999**, *308*, 249−255.

(58) Van Caillie, C.; Amos, R. D. Geometric derivatives of density functional theory excitation energies using gradient-corrected functionals. *Chem. Phys. Lett.* **2000**, *317*, 159−164.

(59) Furche, F.; Ahlrichs, R. Adiabatic time-dependent density functional methods for excited state properties. *J. Chem. Phys.* **2002**, *117*, 7433−7447.

(60) Scalmani, G.; Frisch, M. J.; Mennucci, B.; Tomasi, J.; Cammi, R.; Barone, V. Geometries and properties of excited states in the gas phase and in solution: Theory and application of a time-dependent density functional theory polarizable continuum model. *J. Chem. Phys.* **2006**, *124*, No. 094107.

(61) O'Boyle, N. M.; Tenderholt, A. L.; Langner, K. M. Cclib: A library for package-independent computational chemistry algorithms. *J. Comput. Chem.* **2008**, *29*, 839−845.

(62) Allouche, A.-R. Gabedit—A graphical user interface for computational chemistry softwares. *J. Comput. Chem.* **2011**, *32*, 174−182.

(63) Niu, H.; Huang, Y.; Bai, X.; Li, X.; Zhang, G. Study on crystallization, thermal stability and hole transport properties of conjugated polyazomethine materials containing 4,4′-Bisamine-triphenylamine. *Mater. Chem. Phys.* **2004**, *86*, 33−37.

(64) He, G.; Li, Y.; Liu, J.; Yang, Y. Enhanced electroluminescence using polystyrene as a matrix. *Appl. Phys. Lett.* **2002**, *80*, 4247−4249.

(65) Nedeltchev, A. K.; Han, H.; Bhowmik, P. K. Photoactive amorphous molecular materials based on quinoline amines and their synthesis by Friedländer condensation reaction. *Tetrahedron* **2010**, *66*, 9319−9468.

(66) Granström, M.; Berggren, M.; Pede, D.; Inganäs, O.; Andersson, M. R.; Hjertberg, T.; Wennerström, O. Self organizing polymer films—a route to novel electronic devices based on conjugated polymers. *Supramol. Sci.* **1997**, *4*, 27−34.

(67) Wu, F.; Hsu, S.; Cheng, H.; Chou, W.; Tang, F. Effects of Soft Insulating Polymer Doping on the Photovoltaic Properties of Polymer−Fullerene Blend Solar Cells. *J. Phys. Chem. C* **2013**, *117*, 8691−8696.

(68) Roy, S.; Aguirre, A.; Higgins, D. a.; Chikan, V. Investigation of Charge Transfer Interactions in CdSe Nanorod P3HT/PMMA Blends by Optical Microscopy. *J. Phys. Chem. C* **2012**, *116*, 3153−3160.

(69) Basak, D.; Mallik, B. Detailed Studies on the Photoswitching Property of Ferrocene-Doped Poly(methyl Methacrylate) Thin Films Containing Chloroform Molecules. *Synth. Met.* **2006**, *156*, 176−184.

(70) Yang, D.; Shresths, R. P.; Dingemans, T. J.; Samulski, E. T.; Irene, E. A. Optical properties of N,N′-bis(3-phenoxy-3-phenoxyphenoxy)-1,4,5,8-naphthalene-tetracarboxylic diimide by spectroscopic ellipsometry. *Thin Solid Films* **2006**, *500*, 9−14.

(71) Chen, R.; Zhao, G.; Yang, X.; Jiang, X.; Liu, J.; Tian, H.; Gao, Y.; Liu, X.; Han, K.; Sun, M.; et al. Photoinduced Intramolecular Charge-Transfer State in Thiophene-Π-Conjugated Donor−acceptor Molecules. *J. Mol. Struct.* **2008**, *876*, 102−109.

(72) Wang, H.; Lin, J.; Huang, W.; Wei, W. Fluorescence "turn-On" Metal Ion Sensors Based on Switching of Intramolecular Charge Transfer of Donor−acceptor Systems. *Sens. Actuators, B* **2010**, *150*, 798−805.

(73) Kung, Y.-Ch; Hsiao, S.-H. Solution-processable, high-T_g, ambipolar polyimide electrochromics bearing pyrenylamine units. *J. Mater. Chem.* **2011**, *21*, 1746−1754.

(74) Sek, D.; Bijak, K.; Grucela-Zajac, M.; Filapek, M.; Skorka, L.; Siwy, M.; Janeczek, H.; Schab-Balcerzak, E. Synthesis and study on the light absorbing, emitting, redox and electrochromic properties of azines and polyazines with thiophene units. *Synth. Met.* **2012**, *162*, 1623−1635.

(75) Trasatti, S. The Absolute Electrode Potential: An Explanatory Note. *Pure Appl. Chem.* **1986**, *58*, 955−966.